

# 1 Interferences on Aerosol Acidity Quantification due to Gas-phase Ammonia Uptake onto

## 2 Acidic Sulfate Filter Samples

3 Benjamin A. Nault<sup>1,2,\*</sup>, Pedro Campuzano-Jost<sup>1,2</sup>, Douglas A. Day<sup>1,2</sup>, Hongyu Guo<sup>1,2</sup>, Duseong S.  
4 Jo<sup>1,2,\*\*</sup>, Anne V. Handschy<sup>1,2</sup>, Demetrios Pagonis<sup>1,2</sup>, Jason C. Schroder<sup>1,2,\*\*\*</sup>, Melinda K.  
5 Schueneman<sup>1,2</sup>, Michael J. Cubison<sup>3</sup>, Jack E. Dibb<sup>4</sup>, Alma Hodzic<sup>5</sup>, Weiwei Hu<sup>6</sup>, Brett B. Palm<sup>7</sup>,  
6 Jose L. Jimenez<sup>1,2</sup>

7

8 1. Department of Chemistry, University of Colorado, Boulder, CO, USA

9 2. Cooperative Institute for Research in Environmental Sciences, University of Colorado,  
10 Boulder, CO, USA

11 3. TOFWERK AG, Boulder, CO USA

12 4. Earth Systems Research Center, Institute for the Study of Earth, Oceans, and Space,  
13 University of New Hampshire, Durham, NH, USA

14 5. Atmospheric Chemistry Observations and Modeling Laboratory, National Center for  
15 Atmospheric Research, Boulder, CO, USA

16 6. State Key Laboratory at Organic Geochemistry, Guangzhou, Institute of Geochemistry,  
17 Chinese Academy of Sciences, Guangzhou, China

18 7. Department of Atmospheric Sciences, University of Washington, Seattle, WA, USA

19 \* Now at: Center for Aerosols and Cloud Chemistry, Aerodyne Research, Inc., Billerica, MA,  
20 USA

21 \*\* Now at: Advanced Study Program, National Center for Atmospheric Research, Boulder, CO  
22 USA

23 \*\*\* Now at: Colorado Department of Public Health and Environment, Denver, CO, USA

24

25 Correspondence: Jose L. Jimenez (jose.jimenez@colorado.edu)

26

27 *For submission to Atmospheric Measurement Techniques*

## 28 Abstract

29 Measurements of the mass concentration and chemical speciation of aerosols are important to  
30 investigate their chemical and physical processing from near emission sources to the most  
31 remote regions of the atmosphere. A common method to analyze aerosols is to collect them onto  
32 filters and to analyze filters off-line; however, biases in some chemical components are possible  
33 due to changes in the accumulated particles during the handling of the samples. Any biases  
34 would impact the measured chemical composition, which in turn affects our understanding of  
35 numerous physico-chemical processes and aerosol radiative properties. We show, using filters  
36 collected onboard the NASA DC-8 and NSF C-130 during six different aircraft campaigns, a  
37 consistent, substantial difference in ammonium mass concentration and ammonium-to-anion  
38 ratios, when comparing the aerosols collected on filters versus the Aerodyne Aerosol Mass  
39 Spectrometer (AMS). Another *on-line* measurement is consistent with the AMS in showing that  
40 the aerosol has lower ammonium-to-anion ratios than obtained by the filters. Using a gas uptake  
41 model with literature values for accommodation coefficients, we show that for ambient ammonia  
42 mixing ratios greater than 10 ppbv, the time scale for ammonia reacting with acidic aerosol on  
43 filter substrates is less than 30 s (typical filter handling time in the aircraft) for typical aerosol  
44 volume distributions. Measurements of gas-phase ammonia inside the cabin of the DC-8 show  
45 ammonia mixing ratios of  $45 \pm 20$  ppbv, consistent with mixing ratios observed in other indoor  
46 environments. This analysis enables guidelines for filter handling to reduce ammonia uptake.  
47 Finally, a more meaningful limit-of-detection for SAGA filters collected during airborne  
48 campaigns is  $\sim 0.2 \mu\text{g sm}^{-3}$  ammonium, which is substantially higher than the limit-of-detection  
49 of the ion chromatography. A similar analysis should be conducted for filters that collect  
50 inorganic aerosol and do not have ammonia scrubbers and/or are handled in the presence of  
51 human ammonia emissions.

## 52 Introduction

53 Particulate matter (PM), or aerosol, impacts human health, ecosystem health, visibility,  
54 climate, cloud formation and lifetime, and atmospheric chemistry (Meskhidze et al., 2003;  
55 Abbatt et al., 2006; Seinfeld. and Pandis, 2006; Jimenez et al., 2009; Myhre et al., 2013; Cohen  
56 et al., 2017; Hodzic and Duvel, 2018; Heald and Kroll, 2020; Pye et al., 2020). Quantitative  
57 measurements of the chemical composition and aerosol mass concentration are necessary to  
58 understand these impacts and to constrain and improve chemical transport models (CTMs). The  
59 inorganic portion of aerosol, which includes both volatile (e.g., nitrate, ammonium) and  
60 non-volatile (e.g., calcium, sodium) species, controls many of these impacts through the  
61 regulation of charge balance, aerosol pH, and aerosol liquid water concentration (Guo et al.,  
62 2015, 2018; Hennigan et al., 2015; Nguyen et al., 2016; Pye et al., 2020). Further, the inorganic  
63 portion of aerosol is an important fraction of the aerosol budget, both in polluted cities (e.g.,  
64 Jimenez et al., 2009; Song et al., 2018), and remote regions (e.g., Hodzic et al., 2020), and the  
65 chemistry controlling the inorganic portion of the aerosol is still not well known (e.g., Liu et al.,  
66 2020).

67 There are numerous methods to quantify the inorganic aerosol composition and mass  
68 concentration, including by mass spectrometry (DeCarlo et al., 2006; Canagaratna et al., 2007;  
69 Pratt and Prather, 2010; Froyd et al., 2019), *on-line* ion chromatography (Talbot et al., 1997;  
70 Weber et al., 2001; Nie et al., 2010), and collection onto filters to be extracted and measured  
71 off-line by ion chromatography (Malm et al., 1994; Dibb et al., 2002, 2003; Coury and Dillner,  
72 2009; Watson et al., 2009). Each method has different advantages and disadvantages (e.g., time  
73 resolution, sample preparation, range of species identified, cost, and personnel needs). These

74 results, in turn, have been used to inform and improve the results of CTMs, influencing our  
75 understanding in processes such as the direct radiative effect (Wang et al., 2008b), transport of  
76 ammonia in deep convection (Ge et al., 2018), aerosol pH (Pye et al., 2020; Zakoura et al., 2020)  
77 and subsequent chemistry, and precursor emissions (Henze et al., 2009; Heald et al., 2012;  
78 Walker et al., 2012; Mezuman et al., 2016).

79 Filter measurements have been shown to be most prone to artifacts during sample  
80 collection, handling, storage of the filter, or extraction of the aerosol from the filter prior to  
81 analysis. These artifacts include evaporation of volatile compounds such as organics (Watson et  
82 al., 2009; Chow et al., 2010; Cheng and He, 2015) and ammonium nitrate (Hering and Cass,  
83 1999; Chow et al., 2005; Nie et al., 2010; Liu et al., 2014, 2015; Heim et al., 2020), as well as  
84 chemical reactions of gas-phase species with the accumulated particles (e.g., Schauer et al.,  
85 2003; Dzepina et al., 2007). Further, early research indicated potential artifacts from gas-phase  
86 ammonia uptake onto acidic aerosol collected onto filters, leading to a positive bias for  
87 particulate ammonium (Klockow et al., 1979; Hayes et al., 1980; Koutrakis et al., 1988). This led  
88 to debates about whether aerosol in the lower stratosphere was sulfuric acid or ammonium  
89 sulfate (Hayes et al., 1980); however, after improved filter handling practices and *on-line*  
90 measurements (i.e., mass spectrometry), it has been generally well accepted that the sulfate in the  
91 stratosphere is mainly sulfuric acid (Murphy et al., 2014).

92 This artifact may impact aerosol collected in remote locations (e.g., the lower  
93 stratosphere, but also the free troposphere over the Pacific Ocean basin). Comparisons for a  
94 major cation, ammonium, in a similar location (middle of the Pacific Ocean) have shown very  
95 different results (Dibb et al., 2003; Paulot et al., 2015). This, in turn, affects the observed charge

96 balance of anions (sulfate and nitrate) with ammonium, which can indicate different aerosol  
97 phase state (Colberg et al., 2003; Wang et al., 2008a) and aerosol pH (Pye et al., 2020), leading  
98 to potentially important chemical and physical differences between the real state of the particles  
99 and that concluded from the measurements. An example of the differences in observed charge  
100 balance of ammonium to sulfate for different studies of the same remote Pacific Ocean region is  
101 highlighted in Fig. 1. This difference leads to the inorganic portion of the aerosol potentially  
102 being solid (filters) and hence good ice-nucleating particles (Abbatt et al., 2006), versus it being  
103 liquid (*on-line* measurements), leading to important differences in the calculated radiative  
104 balance. It should be noted that other measurements (both filter and *on-line*) in a similar location  
105 from another study (bar at surface (Paulot et al., 2015)) are more in-line with the *on-line*  
106 observations. A large decrease in the ambient ammonia mixing ratio is required to change from  
107 ammonium sulfate-like aerosols to sulfuric acid-like aerosols between the years, contradictory to  
108 the increasing trends of ammonia globally (Warner et al., 2016, 2017; Weber et al., 2016; Liu et  
109 al., 2019; Tao and Murphy, 2019). Further, oceanic emissions of ammonia are not high enough to  
110 lead to full charge neutralization of sulfate, since these emissions are approximately an order of  
111 magnitude less than those of sulfate precursors (Faloona, 2009; Paulot et al., 2015). A debate  
112 about the acidity and potential impact of ammonia-uptake artifacts on acidic filters for remote  
113 locations has not occurred as it did for stratospheric observations.

114 Previous laboratory studies have suggested that exposure of acidic aerosol, both  
115 suspended in air in a flow tube or on a filter, to gas-phase ammonia will lead to formation of  
116 ammonium salts in short time ( $\leq 10$  s) (Klockow et al., 1979; Huntzicker et al., 1980); however,  
117 it has not been investigated if this time frame applies for acidic aerosol collected on filters

118 handled in a typical indoor environment. Though human emissions of ammonia are variable and  
119 depend on various factors (e.g., temperature, clothing, etc.) (Li et al., 2020), the emissions of  
120 ammonia, specifically from perspiration but also from breath, can lead to high, accumulated  
121 mixing ratios of ammonia indoor (e.g., Ampollini et al., 2019; Finewax et al., 2020) and  
122 references therein), depending on the ventilation rate. The mixing ratios of ammonia can be  
123 factor of 2 to 2000 higher indoor versus outdoor. This higher mixing ratio of ammonia leads to  
124 similarly high mixing ratios used in prior studies to lead to partially to fully neutralize sulfuric  
125 acid (Klockow et al., 1979; Huntzicker et al., 1980; Daumer et al., 1992; Liggio et al., 2011).

126         Here, we investigate whether previously observed laboratory observations of ammonium  
127 uptake to acidic particulate lead to the large differences in ammonium, both in mass  
128 concentration and in ammonium-to-sulfate ratios or ammonium-to-anion ratios, between *in-situ*  
129 measurements and *off-line* filter measurement during five NASA and one NSF airborne  
130 campaigns that sampled air over remote continental and oceanic regions. An uptake model for  
131 gas-phase ammonia interacting with acidic PM on a filter along with constraints from  
132 observations of gas-phase ammonia in the cabin of the airplane are used to further probe the  
133 reason behind the differences between the *in-situ* and *off-line* measurements of ammonium. The  
134 results provide insight into how to interpret prior aircraft measurements and other filter based  
135 measurements where the filters were handled in environments (i.e., indoors), where rapid uptake  
136 of ammonia to acidic PM will occur.

137

## 138 **2. Methods**

### 139 **2.1 Aircraft Campaigns**

140 Five different NASA aircraft campaigns on-board the DC-8 research aircraft and one  
141 NSF aircraft campaign on-board the C-130 research aircraft are used in this study. As described  
142 below, though the campaigns were sampling ambient (outside) air in various locations around the  
143 world, the filters were handled and exposed to both aircraft cabin air and indoor temporary  
144 laboratory air, where between 20 and 40 people were operating instruments. The campaigns  
145 include the Arctic Research of the Composition of the Troposphere from Aircraft and Satellites  
146 (ARCTAS) -A (April 2008) and -B (June – July 2008) campaigns (Jacob et al., 2010), the  
147 Studies of Emissions and Atmospheric Composition, Clouds, and Climate Coupling by Regional  
148 Surveys (SEAC<sup>4</sup>RS, August – September 2013) campaign (Toon et al., 2016), the Wintertime  
149 INvestigation of Transport, Emissions, and Reactivity (WINTER, February – March 2015)  
150 (Schroder et al., 2018), and the Atmospheric Tomography (ATom) -1 (July – August 2016) and  
151 -2 (January – February 2017) campaigns (Hodzic et al., 2020). ARCTAS-A was based in  
152 Fairbanks, Alaska, Thule, Greenland, and Iqaluit, Nunavut, and sampled the Arctic Ocean and  
153 Arctic regions of Alaska, Canada, and Greenland; while, ARCTAS-B was based in Cold Lake,  
154 Alberta, Canada, and sampled the boreal Canadian forest, including wildfire smoke. SEAC<sup>4</sup>RS  
155 was based in Houston, Texas, and sampled biomass burning from western forest fires and  
156 agricultural burns along the Mississippi River and the Southern United States, isoprene  
157 chemistry over Southern United States and midwestern deciduous forests, and deep convection  
158 associated with isolated thunderstorms, the North American Monsoon, and tropical depressions.  
159 Finally, ATom-1 and -2 sampled the remote atmosphere over the Arctic, Pacific, Southern, and  
160 Atlantic Oceans during the Northern (Southern) Hemispheric summer (winter) and winter  
161 (summer).

162 For ARCTAS-A, -B, and SEAC<sup>4</sup>RS, the general sampling scheme was regional, sampling  
163 large regions at level flight tracks. ATom-1 and -2, being global in nature, only sampled at level  
164 legs for short durations (5 – 15 min) at low (~300 m) and high (10 – 12 km) altitude, and did not  
165 measure at level altitudes between the low and high altitude. Due to the sampling time of the  
166 filters (see Sect. 2.2.2), the entirety of the ascent and descent time was needed for one filter  
167 sample. Therefore, all data during the ascents and descents have not been considered in this  
168 study to minimize any issues due to the mixing of aerosols of different compositions and  
169 acidities.

170

## 171 **2.2 Aerosol Measurements**

### 172 **2.2.1 Aerosol Mass Spectrometer**

173 An Aerodyne High-Resolution Time-of-Flight Aerosol Mass Spectrometer, flown by the  
174 University of Colorado-Boulder (CU for short), was flown during the five campaigns used here.  
175 The general features of the AMS have been described in prior studies (DeCarlo et al., 2006;  
176 Canagaratna et al., 2007), and the specifics of the CU AMS for each campaign has been  
177 described elsewhere (Cubison et al., 2011; Liu et al., 2017; Nault et al., 2018; Schroder et al.,  
178 2018; Guo et al., 2020; Hodzic et al., 2020). In brief, the AMS measured the mass concentration  
179 of non-refractory species in PM<sub>1</sub> (PM with an aerodynamic diameter less than 1 μm, see Guo et  
180 al. (2020) for details). Ambient air was sampled by drawing air through an NCAR  
181 High-Performance Instrumental Platform for Environmental Modular Inlet (HIMIL; Stith et al.  
182 (2009)) at a constant standard flow rate of 9 L min<sup>-1</sup> (T = 273.15 K and P = 1013 hPa). The best  
183 estimated upper size cut-off for the HIMIL inlet is ~1 μm diameter (geometric, David Rogers,



pers. comm. 2011). This diameter is larger than the size cut-off than that of the AMS inlet (~0.5-0.7  $\mu\text{m}$  diameter, geometric, depending on the composition), with no losses in the tubing between the HIMIL and AMS inlet expected (see Guo et al. (2020) for more details). Multiple comparisons with instruments sampling from an isokinetic inlet  $\text{PM}_{10}$  inlet (Brock et al., 2019; Guo et al., 2020) indicate that no significant sampling biases were incurred over the size range of the AMS. No active drying of the sampling flow was used to minimize artifacts for semi-volatile species, but the temperature differential between ambient and cabin typically ensured the relative humidity (RH) inside the sampling line less than 40% (e.g., Nault et al., 2018). An exception to this was during ATom-1 and -2, where the cabin temperature, along with the high RH in tropics, led to higher RH in the sample lines in a few instances in the boundary layer, which was accounted for in the final mass concentrations (Guo et al., 2020). To minimize any potential losses of volatile aerosol components, the residence time between the inlet and AMS was less than 1 s (Nault et al., 2018; Schroder et al., 2018; Guo et al., 2020). Prior studies (Guo et al., 2016; Shingler et al., 2016) have shown minimal loss of semivolatile components for this residence time.

The air sample was introduced into the AMS via an aerodynamic focusing lens (Zhang et al., 2002, 2004), which was operated at 2.00 hPa (1.50 Torr), via a pressure-controlled inlet, which was operated at various pressures (94-325 Torr) (Bahreini et al., 2008), depending on the ceiling of the campaign and lens transmission calibrations (Hu et al., 2017b; Nault et al., 2018). The aerosol, once focused, was introduced into a detection chamber after three differential pumping stages. The aerosol impacted on an inverted cone porous tungsten “standard” vaporizer under high vacuum, which was held at  $\sim 600^\circ\text{C}$ . Upon impaction, the non-refractory portion of

206 the aerosol (organic, ammonium, nitrate, sulfate, and chloride) were flash-vaporized, and the  
207 vapors were ionized by 70 eV electron ionization. The ions were then extracted and analyzed  
208 with a H-TOF time-of-flight mass spectrometer (Tofwerk AG). The AMS was operated in the  
209 “V-mode” ion path (DeCarlo et al., 2006), with spectral resolution ( $m/\Delta m$ ) of 2500 at  $m/z$  44 and  
210 2800 at  $m/z$  184. The collection efficiency (CE) for AMS was estimated with the  
211 parameterization of Middlebrook et al. (2012), which has been shown to perform well for  
212 ambient aerosols (Hu et al., 2017a, 2020). The AMS nominally samples aerosol with vacuum  
213 aerodynamic diameter between 40 nm and 1400 nm, which was calibrated for in SEAC<sup>4</sup>RS,  
214 ATom-1, and -2 (Liu et al., 2017; Guo et al., 2020). Mass and/or volumen closure has been  
215 investigated between the AMS and other measurements for all campaigns discussed here  
216 (Cubison et al., 2011; Aknan, 2015; Liu et al., 2017; Nault et al., 2018; Schroder et al., 2018;  
217 Guo et al., 2020). The closure was complete for the size range of the AMS and did not show any  
218 dependence with altitude (Guo et al., 2020). Software packages Squirrel and PIKA under Igor  
219 Pro 7 (WaveMetrics, Lake Oswego, OR) (DeCarlo et al., 2006; Sueper, 2018) were used to  
220 analyze all AMS data.

221 A cryogenic pump, to reduce background of ammonium and organics (Nault et al., 2018;  
222 Schroder et al., 2018), was flown on the AMS for SEAC<sup>4</sup>RS, ATom-1, and -2; but not for  
223 ARCTAS-A and -B. The cryogenic pump lowers the temperature of a copper cylinder  
224 surrounding the vaporizer to ~90 K. This freezes out the background gases and ensures low  
225 detection limits from the beginning of the flight, which is critical since aircraft instruments can  
226 typically not be pumped continuously and hence suffer from high backgrounds at switch-on. The

227  $2\sigma$  accuracy for the AMS for inorganic aerosol is estimated to be 35% (Bahreini et al., 2009; Guo  
228 et al., 2020).

229

### 230 **2.2.2 Aerosol Filters**

231 Fast collection of aerosol particles onto filters during airborne sampling, via the  
232 University of New Hampshire Soluble Acidic Gases and Aerosol (SAGA) technique, has been  
233 described elsewhere (Dibb et al., 2002, 2003), and was flown during the five campaigns  
234 investigated here. Briefly, air is sampled into the airplane via a curved leading edge nozzle (Dibb  
235 et al., 2002). The inlet is operated isokinetically during flight, and typically has a 50% collection  
236 efficiency for aerosol with an aerodynamic diameter of  $4.1\ \mu\text{m}$  (Dibb et al., 2002; McNaughton  
237 et al., 2007), with some altitude dependence (Guo et al., 2020). The lower size cut-offs for  
238 SAGA and AMS are similar (Guo et al., 2020). As discussed by Guo et al. (2020; their Fig. 8)  
239 the difference in mass sampled at the smaller sizes between SAGA and AMS is generally  
240 negligible at all altitudes.

241 Aerosol was collected onto Millipore Fluoropore Teflon filters (90 mm diameter with 1  
242  $\mu\text{m}$  pore size). Collection time was dependent on altitude and estimated mass concentration, but  
243 generally 2 to 3  $\text{sm}^3$  (where  $\text{sm}^3$  is standard  $\text{m}^{-3}$  at temperature = 273 K and pressure = 1013 hPa)  
244 volume of air is collected to ensure detectable masses of species (Dibb et al., 2002). The aerosol  
245 inlet flow is close to 400 slpm in the marine boundary layer and approximately 150 slpm at  
246 maximum altitude. Further, 2 blank filters are collected each flight. The filters were contained in  
247 a Delrin holder during collection. After collection, the filters were transferred to a particle free  
248 polyethylene “clean room” bag, which was filled with zero air, sealed, and stored over dry ice.

249 No acid scrubbers were inserted into the bags to prevent any artifact from offgassing of  
250 ammonia. The samples from the filters were then extracted during non-flight days with 20 mL  
251 ultrapure water and preserved with 100  $\mu$ L chloroform (see Sect. S2). The preserved samples  
252 were sent to the University of New Hampshire, to be analyzed by ion chromatography. The  
253 estimated limit of detection for both sulfate and ammonium is  $0.01 \mu\text{g sm}^{-3}$  for all missions  
254 evaluated here (Dibb et al., 1999).

255

### 256 **2.2.3 Other Aerosol Measurements**

257 The NOAA Particle Analysis by Laser Mass Spectrometer (herein PALMS) was flown  
258 during ATom-1 and -2. Details of the PALMS instrument configured for ATom-1 and -2 are  
259 described in Froyd et al. (2019). Briefly, PALMS measures the chemical composition of single  
260 aerosol particles via laser-ablation/ionization (Murphy and Thomson, 1995; Thomson et al.,  
261 2000), where the ions are extracted and detected by a time of flight mass spectrometer. The  
262 instrument measures particles between 100 nm and  $4.8 \mu\text{m}$  (geometric diameter) (Froyd et al.,  
263 2019). The measurement of PALMS used in this study is the “sulfate acidity indicator” (Froyd et  
264 al., 2009). These authors reported that in the negative ion mode, there is a prominent peak at  $m/z$   
265 97, corresponding to  $\text{HSO}_4^-$ , and another peak at  $m/z$  195, corresponding to the cluster  
266  $\text{HSO}_4^-(\text{H}_2\text{SO}_4)$ . The first peak was independent of acidity; whereas, the second peak was  
267 dependent on acidity. Froyd et al. (2009) calibrated the PALMS ratio of  
268  $\text{HSO}_4^-(\text{H}_2\text{SO}_4)/(\text{HSO}_4^- + \text{HSO}_4^-(\text{H}_2\text{SO}_4))$  to Particle-into-Liquid Sampler (PILS) measurements to  
269 achieve an estimate of ammonium balance.

270 Besides the chemical composition, the particle number and volume distributions are used  
271 here. For SEAC<sup>4</sup>RS, the measurements have been described elsewhere (e.g., Liu et al., 2016).  
272 The laser aerosol spectrometer (from TSI), which measured aerosol from geometric diameter 100  
273 nm to 6.3  $\mu\text{m}$ , is used here for volume distribution. For the ATom missions, the measurements  
274 have been described elsewhere (Kupc et al., 2018; Williamson et al., 2018; Brock et al., 2019).  
275 Briefly, the dry particle size distribution, from geometric diameter of 2.7 nm to 4.8  $\mu\text{m}$ , were  
276 measured by a series of optical particle spectrometers, including the Nucleation Model Aerosol  
277 Size Spectrometer (3 nm to 60 nm, custom built (Williamson et al., 2018)), an Ultra-High  
278 Sensitivity Aerosol Spectrometer (60 nm to 1  $\mu\text{m}$ ) from Droplet Measurement Technologies  
279 (Kupc et al., 2018), and Laser Aerosol Spectrometer (120 nm to 4.8  $\mu\text{m}$ ) from TSI). These  
280 measurements have been split in nucleation mode (3 to 12 nm), Aitken mode (12 to 60 nm),  
281 accumulation mode (60 to 500 nm) and coarse mode (500 nm to 4.8  $\mu\text{m}$ ).

282

## 283 **2.3 Gas-Phase and Other Measurements**

### 284 **2.3.1 Ammonia Measurements**

285 Gas-phase ammonia was measured inside the cabin of the NASA DC-8 during the  
286 FIREX-AQ campaign (Warneke et al., 2018), a subsequent DC-8 campaign which shared many  
287 instrument installations and a similar level of aircraft personnel with the campaigns analyzed  
288 here. The location of the instrument and where it sampled cabin ammonia (in relation to where  
289 the SAGA filters are located) is shown in Fig. S1. Ammonia was measured by a Picarro G2103  
290 Gas Concentration Analyzer (von Bobruzki et al., 2010; Sun et al., 2015; Kamp et al., 2019).  
291 The instrument is a continuous, cavity ring-down spectrometer. Cabin air is brought into a cavity

292 at low pressure (18.7 kPa, 140 Torr), where laser light is pulsed into the cavity. The light is  
293 reflected by mirrors in the cavity, providing an effective path length of kilometers. A portion of  
294 the light penetrates the mirrors, reaching the detectors, where the intensity of the light is  
295 measured to determine the mixing ratio of ammonia from the time decay of the light intensity via  
296 Beer-Lambert Law. The instrument measures the absorption of infrared light from 6548.5 to  
297 6549.2  $\text{cm}^{-1}$  (Martin et al., 2016). Absorption of gas-phase water is also measured and corrected  
298 for. This water vapor measurement is also used to calculate RH inside the cabin of the DC-8  
299 (Filges et al., 2018). Data was logged at 1 Hz.

300

### 301 **2.3.2 Carbon Dioxide and Temperature Measurements**

302 Carbon dioxide inside the cabin of the NASA DC-8 during FIREX-AQ was measured by  
303 a HOBO MX1102 Carbon Dioxide Data Logger (HOBO by Onset). It is a self-calibrating carbon  
304 dioxide sensor with a range of 0 to 5,000 ppm carbon dioxide and an accuracy of  $\pm 50$  ppm. A  
305 non-dispersive infrared sensor is used to measure carbon dioxide. Data was acquired once every  
306 10 s to once every 2 min. Besides carbon dioxide, RH and temperature are also recorded by the  
307 instrument. Prior to each flight, the instrument was turned on and measured ambient carbon  
308 dioxide, outside the cabin of the DC-8, to ensure the accuracy of the instrument compared to  
309 ambient carbon dioxide measurements.

310 Ambient carbon dioxide during FIREX-AQ was measured by an updated version of the  
311 instrument known as Atmospheric Vertical Observations of  $\text{CO}_2$  in the Earth's Troposphere  
312 (AVOCET) (Vay et al., 2003, 2011). The updated instrument used a modified LI-COR model  
313 7000 non-dispersive infrared spectrometer and measured carbon dioxide at 5 Hz.

314 Temperature in the cabin was measured by a thermocouple (SEAC<sup>4</sup>RS) or thermistor  
315 (ATom-1 and 2) located in the AMS rack or a Vaisala probe located at the front of the airplane  
316 (ARCTAS-A, -B, and SEAC<sup>4</sup>RS).

317

## 318 **2.4 Theoretical Ammonia Flux Model**

319 To investigate the possibility that the ammonia mixing ratio in the cabin of the DC-8 is  
320 high enough to be taken up by acidic PM on a filter during the short time the filter is exposed to  
321 cabin air prior to final storage, a theoretical uptake model was constructed to estimate the time  
322 scale for ammonia to interact with all the acidic particles (Seinfeld. and Pandis, 2006). The  
323 equations used for the model can be found in the Supplemental Information (Sect. S3). The  
324 model was initialized with a range of ammonia mixing ratios (1 to 200 ppb) and a range of PM  
325 diameters (10 to 1000 nm). The calculations were conducted at 298 K, which is within  $\pm 10$  K of  
326 typical temperatures inside the cabin of the NASA DC-8 during the five campaigns (Fig. S2). An  
327 accommodation coefficient of 1 for ammonia onto acidic PM was assumed (Hanson and  
328 Kosciuch, 2003), with a density of  $1.8 \text{ g cm}^{-3}$  for sulfuric acid (Rumble, 2019). For the mass  
329 transfer calculations, the transition regime (between the free molecular and continuum regimes)  
330 equations were used, using the Fuchs and Sutugin parameterization (Fuchs and Sutugin, 1971).  
331 The model was used to estimate the ammonia molecular flux to acidic PM on the filter (Eq. S3).  
332 Finally, the molecular flux was used to estimate the time it would take all the particles to be  
333 partially neutralized by ammonia in the cabin (Eq. S4), though this may be a lower limit  
334 (Robbins and Cadle, 1958; Daumer et al., 1992).

335

### 336 3. Results and Discussion

#### 337 3.1 Comparison of On-Line and Off-Line Ion Balances across the Tropospheric Column

338 SAGA and AMS co-sampled aerosols during multiple aircraft campaigns. Nitrate quickly  
339 evaporates from aerosols as the aerosols are transported away from source regions and is  
340 typically small in the global troposphere (DeCarlo et al., 2008; Hennigan et al., 2008; Hodzic et  
341 al., 2020). Thus, in Fig. 2 the mass concentrations for the two most important submicron  
342 contributors to ammonium balance, ammonium and sulfate, are compared from the aircraft  
343 campaigns. The campaigns generally sampled remote air, either continental or oceanic, except  
344 for biomass burning sampled during ARCTAS-B and SEAC<sup>4</sup>RS and downwind of urban areas  
345 during WINTER. The measurements, for mass concentrations greater than  $0.1 \mu\text{g sm}^{-3}$ , are  
346 generally within the combined uncertainties of the two instruments. Sulfate generally remains on  
347 the one-to-one line, even at low mass concentrations. However, ammonium shows a large  
348 divergence between the two measurements for mass concentrations less than  $0.1 \mu\text{g sm}^{-3}$  during  
349 all six aircraft campaigns. As shown in Fig. 2, the divergence in ammonium occurs well above  
350 the limit-of-detection for both instruments, namely  $\sim 4 \text{ ng sm}^{-3}$  for AMS for a 5-minute average  
351 (DeCarlo et al., 2006; Guo et al., 2020) and  $10 \text{ ng sm}^{-3}$  for SAGA (Dibb et al., 1999), for both  
352 ammonium and sulfate.

353 This divergence in ammonium mass concentration is thus reflected in the ammonium  
354 balance, defined as the ratio of ammonium to sulfate plus nitrate, in moles (Fig. 3). For all  
355 campaigns, the two measurements show differences in ammonium balance, especially at higher  
356 altitudes, where the aerosols is distant from ammonia emissions (Dentener and Crutzen, 1994;  
357 Paulot et al., 2015), but sulfate production can continue due to vertical transport of precursors



358 such as SO<sub>2</sub>. On average, the SAGA measurements indicate ammonium balance rarely below 0.5  
359 throughout the troposphere; whereas, the AMS measurements indicate that ammonium balance  
360 generally drops to below 0.2 for pressures less than 400 hPa. Fig. 2 and Fig. 3 indicate either  
361 differences in the ammonium balance due to differences in aerosols population sampled, as  
362 SAGA measures larger aerosols diameters than AMS (Guo et al., 2020), or potential artifacts  
363 with one of the measurements.

364 Both the AMS and the filters sample most of the submicron aerosols (see Guo et al.  
365 (2020) for details), but the filters also sample supermicron particles that the AMS does not.  
366 Therefore it is possible in principle that the difference could be due to ammonium present in  
367 supermicron particles. As discussed in Guo et al. (2020), nearly 100% of the measured volume  
368 occurs for aerosols < 1 µm above the marine boundary layer, where the largest difference in  
369 ammonium balance between the filters and AMS occurs (Fig. 3). Further, ammonium has been  
370 observed to be a small fraction of the supermicron mass (Kline et al., 2004; Cozic et al., 2008;  
371 Pratt and Prather, 2010), except for instances of continental fog (Yao and Zhang, 2012) and  
372 Asian dust events (Heim et al., 2020). An upper estimate of supermicron ammonium can be  
373 calculated using results from prior studies (Kline et al., 2004; Cozic et al., 2008). In these prior  
374 studies, ~90% of the ammonium was submicron. With the average ammonium observed during  
375 ATom-1 and -2 (~10 to 50 ng sm<sup>-3</sup>) (Hodzic et al., 2020), that would suggest an upper limit of ~1  
376 to 5 ng sm<sup>-3</sup> ammonium in the supermicron aerosols. This upper estimate does not explain the  
377 differences between AMS and filters during ATom-1 and -2 (Fig. S3), as the percent difference  
378 increases with decreasing estimated supermicron ammonium volume. As the largest differences  
379 between the AMS and filters occur well above the boundary layer (Fig. 3), away from

380 continental ammonia sources (Dentener and Crutzen, 1994) and Asian dust events, we conclude  
381 that the sampling of supermicron aerosols by filters is not leading to the observed differences in  
382 ammonium.

383         The only useful comparison, other than SAGA versus AMS, is with PALMS during  
384 ATom. Prior studies by PALMS have shown aerosols observed for pressure < 400 hPa to be  
385 acidic, depending on potential recent influence of boundary layer air via convection (Froyd et al.,  
386 2009; Liao et al., 2015), similar to observations by other single particle mass spectrometers (Pratt  
387 and Prather, 2010). Though not reaching similarly low  $\text{NH}_4/(2\times\text{SO}_4)$  values as the AMS, the  
388 PALMS acidity marker shows much lower values than were determined by the aerosols collected  
389 on the filters (Fig. S4). Different reasons for PALMS not achieving as low values as AMS may  
390 include differences in aerosols sizes sampled by PALMS versus AMS (Guo et al., 2020), and the  
391 sensitivity of the acidity marker to laser power (Liao et al., 2015). Thus, two different *on-line*  
392 measurements indicate that the ammonium balance is lower than the aerosols collected on filters,  
393 suggesting potentially more acidic aerosols.

394         Differences in ammonium balance between AMS and SAGA are detectable for sulfate  
395 mass concentrations  $\leq 1 \mu\text{g sm}^{-3}$  (Fig. 4) for all six aircraft campaigns. As the sulfate mass  
396 concentration decreases, the relative differences in ammonium, and thus ammonium balance,  
397 increase. The large majority of the troposphere contains sulfate mass concentrations in which the  
398 differences in ammonium are observed, highlighting the importance of this problem (Fig. 4a).  
399 Thus, except for more polluted conditions ( $> 1 \mu\text{g sm}^{-3}$  sulfate), which mainly occurs in  
400 continental (Jimenez et al., 2009; Kim et al., 2015; Malm et al., 2017) and urban regions  
401 (Jimenez et al., 2009; Hu et al., 2016; Kim et al., 2018; Nault et al., 2018), this bias between

402 filters and *on-line* measurements is critically important, especially since airborne measurements  
403 are often the only meaningful observational constraints for remote regions. Thus, this analysis  
404 suggests that for SAGA filters, a more meaningful ammonium limit-of-detection would be  
405 equivalent to  $1 \mu\text{g sm}^{-3}$  sulfate, which would be  $\sim 0.2 \mu\text{g sm}^{-3}$  ammonium. This also provides the  
406 framework to define limit-of-detection for other filter-based measurements not associated with  
407 ion chromatography.

408

### 409 **3.2 Ammonia Levels on the NASA DC-8 Cabins**

410 Prior studies have suggested that various sources of ammonia could impact acidic filter  
411 measurements (Klockow et al., 1979; Hayes et al., 1980; Koutrakis et al., 1988). Some of these  
412 studies found that the materials of the containers where the filters are stored, unless thoroughly  
413 cleaned and not stored around humans, are a source of ammonia gas that reacts with the sulfuric  
414 acid on the filters to become ammonium, leading to ammonium bisulfate or ammonium sulfate  
415 (Hayes et al., 1980). Further, handling of acidic filters in rooms with people or acidic aerosol in  
416 the presence of human breath can also lead to near to complete neutralization of acidic aerosol  
417 (Larson et al., 1977; Hayes et al., 1980; Clark et al., 1995). Finally, various studies have  
418 suggested that the SAGA filters specifically may be impacted by various ammonia sources prior  
419 to sampling with the ion chromatography (Dibb et al., 1999, 2000; Fisher et al., 2011).

420 During SAGA sampling, the filters with collected aerosol are moved from the sample  
421 collector to a polyethylene bag that is filled with clean air. During this step, the filter is exposed  
422 to the cabin air of the DC-8 for  $\sim 10$  s. As humans are a source of ammonia (Larson et al., 1977;  
423 Clark et al., 1995; Sutton et al., 2000; Finewax et al., 2020; Li et al., 2020), this source sustains

424 significant ammonia concentrations in indoor environments, which could potentially bias the  
425 filter measurements. *On-line* measurements would not be subject to this effect since the sampled  
426 air is not exposed to cabin air before measurement. While inlet lines for *on-line* instruments  
427 could in theory lead to some memory effects, there is no evidence of such effects in the data  
428 (e.g., the response going from a large, neutralized plume into the acidic FT is nearly  
429 instantaneous (Schroder et al., 2018)).

430       During a recent 2019 NASA DC-8 aircraft campaign, FIREX-AQ, ammonia was  
431 measured on-board the DC-8 during several research flights. An example time series of cabin  
432 ammonia, temperature, and RH is shown in Fig. 5. Prior to take-off, as scientists were slowly  
433 boarding the airplane, the ammonia mixing ratio was low ( $< 20$  ppbv) and similar to ambient  
434 levels of ammonia outside the aircraft. As scientists started boarding before take-off, the  
435 ammonia mixing ratio increased. Upon doors closing, the mixing ratio leveled off at  $\sim 40$  ppbv.  
436 After take-off, the mixing ratio remained  $\sim 40$  ppbv, though there were changes related to  
437 changes in cabin temperature and humidity, which would affect emission rates and also  
438 adsorption of ammonia onto cabin surfaces (Sutton et al., 2000; Finewax et al., 2020; Li et al.,  
439 2020) and movement of scientists throughout the cabin, which would affect emission rates and  
440 their location.

441       The average ( $\pm 1\sigma$  spread of the observations) and median ammonia in the cabin of the  
442 DC-8 during FIREX-AQ was  $45.4 \pm 19.9$  and 41.9 ppbv (Fig. 6). There was a large positive tail in  
443 ammonia mixing ratio, related to high temperatures (Fig. S5), which causes the scientists to  
444 perspire more and release more ammonia (Sutton et al., 2000; Finewax et al., 2020; Li et al.,  
445 2020). Compared to outdoor ammonia mixing ratios, ranging from urban to remote locations, the

446 ammonia in the cabin of the DC-8 is higher by a factor of 2 to 2000 (Fig. 6). On the other hand,  
447 the ammonia measured in the cabin of the DC-8 is similar but towards the lower end of the  
448 mixing ratios measured during various indoor studies (Table S1 for compilation of references).

449         The ammonia mixing ratios observed in the cabin were verified by investigating the cabin  
450 air exchange rates (see SI Sect. S3). Using carbon dioxide measurements, the exchange rate in  
451 the cabin was calculated to be  $9.9 \text{ hr}^{-1}$  (Fig. S6), which is similar to literature values for the cabin  
452 exchange rate of other passenger airliners (Hunt and Space, 1994; Hocking, 1998; Brundrett,  
453 2001; National Research Council, 2002). This value is a factor of 2 to 5 higher than typical  
454 exchange rates for commercial buildings (Hunt and Space, 1994; Pagonis et al., 2019), which  
455 would suggest lower mixing ratios than observed in other indoor environments. Using this  
456 exchange rate, and the literature total ammonia emission rates from humans ( $1940 \mu\text{g hr}^{-1}$   
457  $\text{person}^{-1}$  (Sutton et al., 2000)) and the average of ambient ammonia mixing ratios as an outdoor  
458 background onto which the human emissions in the cabin are added ( $\sim 4.4 \text{ ppbv}$ , Fig. 6), the  
459 ammonia mixing ratio in the cabin of the DC-8 was estimated to be  $43.4 \text{ ppbv}$ , which is within  
460 the uncertainty of the average ammonia ( $45.4 \pm 19.9 \text{ ppbv}$ ) inside the cabin of the DC-8. Thus, the  
461 observed ammonia mixing ratios in the cabin of the DC-8 are consistent with the cabin air  
462 exchange rates and literature human ammonia emissions. These mixing ratios are approximately  
463 a factor of nine higher than in a typical laboratory environment (Fig. S7), as there are fewer  
464 people (1 to 4 versus 20 to 40), making the cabin of the DC-8 an extreme laboratory environment  
465 for handling acidic filters. As shown in Fig. 6, ammonia mixing ratios in indoor environments  
466 are high enough to change the thermodynamics of inorganic aerosol, leading to higher  
467 ammonium balances (Weber et al., 2016). Thus, similar to the conclusions of other studies, the

468 cabin of the DC-8 is an important source of ammonia that could lead to biases with acidic  
469 aerosols collected on filters.

470 During FIREX-AQ, the DC-8 frequently sampled air impacted by biomass burning,  
471 which is an important source of ammonia (Sutton et al., 2013) and could potentially increase the  
472 background ammonia being brought into and mixing with the cabin air being sampled by the  
473 Picarro. Splitting the cabin ammonia ratios between sampling air impacted by biomass burning  
474 versus nominally background air, the normalized PDF did not shift to higher ammonia mixing  
475 ratios (Fig. S7). Further, the averages of the observed cabin ammonia was statistically similar, at  
476 the 95% confidence interval, between the DC-8 sampling biomass burning and nominally  
477 background air ( $48.1 \pm 13.4$  versus  $44.1 \pm 14.4$  ppbv for biomass burning and background air,  
478 respectively). Finally, the majority of the time the cabin air was sampled by the Picarro for cabin  
479 ammonia, the DC-8 was sampling agricultural fires in Southeast US, which are shorter in  
480 duration (seconds) versus the large wildfires in Western US (minutes to hours). This is reflected  
481 in the low average ambient value for ammonia, as measured by a proton transfer reaction mass  
482 spectrometer (Müller et al., 2014), when the DC-8 was sampling biomass burning-influenced air  
483 observed during this time ( $\sim 10$  ppbv) and very low average value for non-biomass  
484 burning-influenced air ( $\sim 0.8$  ppbv) (Fig. S7). Thus, ammonia from biomass burning would at  
485 most be a small impact on the ammonia measured in the cabin of the DC-8, further indicating the  
486 ammonia in the cabin was mainly from human emissions.

487

### 488 **3.3 Can Uptake of Cabin Ammonia Explain the Higher Ammonium Concentrations on** 489 **Filters?**

490 As shown in Fig. 6, the cabin of the DC-8 is an important source of ammonia from the  
491 breathing and perspiring of scientists. Prior studies (Klockow et al., 1979; Huntzicker et al.,  
492 1980; Daumer et al., 1992; Liggio et al., 2011) have shown in laboratory settings that 10 s is fast  
493 enough to partially to fully neutralize sulfuric acid. Thus, here we investigate whether the time of  
494 the filter handling of 10 s will lead to partial to full neutralization of sulfuric acid from cabin  
495 ammonia, or whether this time is fast enough to limit exposure of the acidic filter to cabin  
496 ammonia. Huntzicker et al. (1980) showed that for typical aerosol modal distributions (Fig. 7)  
497 and cabin RH (Fig. S9), an initial pure sulfuric acid aerosol, suspended in a flow reactor, reaches  
498 equal molar amounts of ammonium and sulfate (i.e., ammonium bisulfate) when exposed to 70  
499 ppb ammonia in 10 s. This indicates the plausibility that acidic aerosol filters, which typically  
500 have lower sulfate mass concentrations than Huntzicker et al. (1980) ( $\sim 2 \mu\text{g}$  versus  $\sim 55 \mu\text{g}$   
501 sulfate equivalent on filters), would interact with cabin ammonia to form at least ammonium  
502 bisulfate. Further, other studies found that in less than 10 s, sulfuric acid aerosol, suspended in a  
503 flow reactor, at  $\text{RH} \leq 45\%$ , will completely react with gas-phase ammonia to form ammonium  
504 sulfate (Robbins and Cadle, 1958; Daumer et al., 1992). The latter study used ammonia mixing  
505 ratios similar to the amount observed in the cabin of the DC-8 ( $\sim 30 \text{ ppbv}$ ); whereas, the former  
506 study used excess ammonia ( $\sim 9 \text{ ppmv}$ ). Some studies have suggested that the bags used to store  
507 the filters may be a source of ammonia (e.g., Hayes et al., 1980); however, calculations indicate  
508 the bags would be a small source of ammonia (see Sect. S4).

509 First, the time of diffusion of ammonia gas from the surface to the interior of the filter  
510 was investigated, as there is a potential for the PM to be embedded deep into the filter. Eq. 1  
511 (Seinfeld. and Pandis, 2006):

$$\tau_{diffusion} = \frac{d_t^2}{8D_g} \quad \text{Eq. 1}$$

where  $d_t^2$  is the depth of the Teflon ( $\sim 0.015$  cm) and  $D_g$  is the diffusion coefficient of ammonia in air ( $0.228 \text{ cm}^2 \text{ s}^{-1}$ ) (Spiller, 1989). Therefore, the estimated timescale for ammonia to diffuse through the depth of the Teflon filter is  $\sim 1 \times 10^{-4}$  s, meaning that the surface of PM will always be in contact with cabin-level mixing ratios of ammonia. Even though the filters have a porous membrane, for molecular diffusion, the membrane only increases the pathway that the ammonia molecules have to travel slightly; thus, not changing the estimated time. Second, as the particles are liquid (Wilson, 1921), the diffusion will be similar as through water. A typical value for diffusivity in water is  $\sim 1 \times 10^{-5} \text{ cm}^2 \text{ s}^{-1}$  (Seinfeld. and Pandis, 2006). For the size ranges observed (Fig. 7,  $\sim 40 - 700$  nm), this corresponds to a timescale of  $1.6 \times 10^{-7}$  to  $5.0 \times 10^{-5}$  s. Thus, the diffusion through the filter and through the PM is nearly instantaneous for ammonia.

A theoretical uptake model for ammonia to acidic PM on filters was run for a range of ammonia mixing ratios and PM diameters (Fig. 7). As shown in Fig. 7, only at the lowest ammonia mixing ratios ( $< 10$  ppbv), the flux of ammonia to acidic PM is slower ( $> 20$  s) than the typical filter handling time ( $\sim 10$  s) for typical aerosol diameters in the remote atmosphere. For the conditions of the DC-8, similar to other indoor environments ( $> 20$  ppbv ammonia, Fig. 6), and ambient aerosol diameters in the accumulation mode that contains most ambient sulfate (Fig. 7), the amount of time needed for cabin ammonia to interact with acidic PM on filters to form ammonium bisulfate is  $\leq 10$  s, similar to the results of Huntzicker et al. (1980). Also, studies show that the kinetic limitation to form ammonium sulfate  $((\text{NH}_4)_2\text{SO}_4)$  versus ammonium bisulfate  $(\text{NH}_4\text{HSO}_4)$  is relatively low and can occur within the 10 s time frame (Robbins and Cadle, 1958; Daumer et al., 1992). A laboratory setting with  $\sim 5$  ppbv  $\text{NH}_3$  would



534 result in the filters needing to be exposed to laboratory air for at least 40 s to form ammonium  
535 bisulfate (Fig. S8) versus the 3 to 10 s for conditions in the cabin of the DC-8 (Fig. 7), further  
536 exemplifying the challenging conditions of the DC-8 cabin for filter sampling.

537         The prior analysis made the assumption that the PM maintained a spherical shape upon  
538 impacting the Teflon filter. More viscous (i.e., solid) PM is more likely to maintain a spherical  
539 shape on filters whereas less viscous (i.e., liquid) PM will spread and become more similar to  
540 cylindrical shape (e.g., Slade et al., 2019). As more acidic aerosol is more likely to be liquid  
541 (e.g., Murray and Bertram, 2008), an exploration of cylindrical shape was conducted. Depending  
542 on the assumed height of the cylindrical shape, the timescale for a molecule of ammonia to  
543 interact with a molecule of sulfuric acid decreases from ~5 s (for maximum ammonia and  
544 aerosol volume) to ~4 s (assuming height of cylinder equals radius of sphere) to less than 1 s as  
545 height decreases from 25 nm or less. The aerosol deforming and spreading upon impacting the  
546 filters increases the particle surface area, and decreases the amount of time for cabin ammonium  
547 to interact with the acidic PM. Thus, less viscous aerosol has more rapid uptake and interaction  
548 with ammonia due to the higher surface area.

549         A potential limitation to the model is the accommodation coefficient of ammonia to  
550 acidic PM, as there are conflicting reports on its value (Hanson and Kosciuch, 2004; Worsnop et  
551 al., 2004). However, as shown in Worsnop et al. (2004), once the sulfuric acid weight percentage  
552 is 50% or greater, the different studies converge to an accommodation coefficient of ~1. Various  
553 studies indicate that the RH in the cabin of jet airplanes is low due to how air is brought into the  
554 airplane, typically < 20% (Hunt and Space, 1994; Brundrett, 2001; National Research Council,  
555 2002). Even though the ambient RH may be higher than the RH in the cabin of the DC-8, the

556 water equilibration is rapid ( $< 1$  s) for the temperature of the cabin of the DC-8, even for very  
557 viscous aerosol (Shiraiwa et al., 2011; Price et al., 2015; Ma et al., 2019), meaning the PM on the  
558 filter would rapidly reach equilibrium with the cabin RH upon exposure. This would result in a  $\geq$   
559 60% sulfuric acid weight percentage (Wilson, 1921) for the typical RH ranges in the cabin of  
560 typical airlines. However, various measurements in the DC-8 cabin indicate the RH is  $\leq 40\%$   
561 (Fig. S9), leading to sulfuric acid weight percentage of 50% or greater (Wilson, 1921).  
562 Therefore, the accommodation coefficient of  $\sim 1$  is well-constrained by the literature. Thus, the  
563 handling of the filters between the sampling inlet to the polyethylene bag exposes the acidic PM  
564 to enough gas-phase ammonia towards forming ammonium bisulfate or ammonium sulfate,  
565 biasing high ammonium from the filters. This explains the differences seen in Fig. 1 – Fig. 4.

566 Another potential limitation is that the PM on the filters could form a layer, as multiple  
567 particles pile up on top of each other, slowing the diffusion of ammonia to be taken up by acidic  
568 PM. The filters have a one-sided surface area of  $6.4 \times 10^{-3} \text{ m}^2$ , while an individual particle at the  
569 mode of the volume distribution (Fig. 7) has a projected surface area of  $\sim 7.1 \times 10^{-14} \text{ m}^2$ . Thus,  
570  $\sim 9.0 \times 10^{10}$  particles would need to be collected to form a single layer of PM on the filter. The  
571 number of molecules in a single particle of the mode size is  $\sim 1.4 \times 10^8$  molecules (Eq. S2).  
572 Therefore,  $\sim 1.3 \times 10^{19}$  molecules need to be collected onto the filters in order to form a monolayer  
573 of PM, which is equivalent to  $\sim 2.2 \times 10^3 \text{ } \mu\text{g}$  total aerosol collected or  $\sim 700 \text{ } \mu\text{g sm}^{-3}$  aerosol  
574 concentration. As the mass concentration in ATom was typically  $\sim 1 \text{ } \mu\text{g sm}^{-3}$  (Hodzic et al.,  
575 2020), and total aerosol concentrations that high is rarely seen except for extreme events (such as  
576 the thickest fresh wildfire plumes), it is very unlikely that more particle layering would delay the  
577 diffusion of ammonia to acidic PM.

578 Various sensitivity analyses of the uptake of ammonia to sulfuric acid were conducted.  
579 First, there is minimal impact of cabin temperature on the results. Though there was a 25 K range  
580 in cabin temperature (Fig. S2), the impact on the molecular speed of ammonia in the model  
581 (Eq. S1) leads to a  $\pm 2\%$  change in molecular speed, resulting in small changes in the time.  
582 Further, only large changes in the accommodation coefficient with temperature occurs for  
583 sulfuric acid weight percentages  $< 40\%$  (Swartz et al., 1999), which is smaller than the weight  
584 percentage expected for the filters in the cabin of the DC-8. For the temperature range of the  
585 cabin of the DC-8 (Fig. S2), the coefficient changes by less than 10%, which leads to a total  
586 maximum change in Fig. 7 of  $\pm 12\%$ . The largest impact on the results in Fig. 7 is changing the  
587 accommodation coefficient. Reducing the accommodation coefficient by a factor of 10, though  
588 not representative of the DC-8 cabin conditions, would mean the acidic PM would need to be  
589 exposed to ammonia for  $\geq 1$  minute (Fig. S10). It is expected that the lower accommodation  
590 coefficient will occur for conditions with higher RH ( $> 80\%$ ), suggesting typical laboratory  
591 conditions (along with the lower ammonia mixing ratios) or ambient conditions may experience  
592 lower ammonia uptake to acidic PM. Finally, organic coatings may impact the accommodation  
593 coefficient of ammonia to sulfuric acid; however, the amount of reduction on the accommodation  
594 coefficient has varied among studies (e.g., Daumer et al., 1992; Liggio et al., 2011). Daumer et  
595 al. (1992) showed no impact; whereas, Liggio et al. (2011) found a similar impact to reducing the  
596 accommodation coefficient by a factor of 10 (Fig. S10). Thus, the results in Fig. 7 are in line  
597 with Daumer et al. (1992) while the results in Fig. S10 are in line with Liggio et al. (2011).

598

### 599 **3.4 Impacts of Ammonia Uptake on Acidic Filters**

600 As discussed throughout this study, uptake of cabin ammonia during the handling of  
601 acidic filters can lead to biases in ammonium mass concentrations. However, other potential  
602 sources of biases include the material used for sampling and storing the filter (Hayes et al.,  
603 1980), and the preparation of the filter in the field to be sampled by ion chromatography. As the  
604 preparation of the filters occurs indoors, as well, the filters will be exposed to similar ammonia  
605 mixing ratios to those shown in Fig. 6.

606 Further, filter collection of aerosols is a widely used technique outside of aircraft  
607 campaigns, including for regulatory purposes and long-term monitoring at various locations  
608 around the world. For many of these sites, ammonia denuders are used to minimize biases of  
609 ammonium on filters (e.g., Baltensperger et al., 2003). Data from remote, high altitude locations  
610 have indicated that the ammonium balance is less than one (Cozic et al., 2008; Sun et al., 2009;  
611 Freney et al., 2016; Zhou et al., 2019), similar to the observations from the AMS shown in  
612 Fig. 3. However, this is dependent on air mass origin and type (Cozic et al., 2008; Sun et al.,  
613 2009; Fröhlich et al., 2015). Thus, sampling of remote aerosols with filters does provide  
614 evidence of ammonium balances less than one due to a combination of procedures to minimize  
615 interaction of gas-phase ammonia with the acidic filters and the lower human presence (and  
616 potentially cooler temperatures at high, remote, mountaintop locations such as Jungfraujoch).

617 However, there are some long-term monitoring stations that do not use denuders or other  
618 practices to minimize the interaction of ammonia with acidic aerosols. For example, the Clean  
619 Air Status and Trends Network (CASTNET), which is located throughout the continental United  
620 States, measures ammonium, sulfate, and nitrate (Solomon et al., 2014). The CASTNET system  
621 uses an open-face system to collect aerosols on Teflon filters for approximately one week for

each filter (Lavery et al., 2009). In comparison, the Chemical Speciation Monitoring Network (CSN), which also samples the continental United States and collects the aerosols on Nylon or Teflon filters, a denuder is used to scrub gas-phase ammonia to minimize interaction of ammonia with acidic aerosols on filters (Solomon et al., 2000, 2014). The comparison between these two long-term monitoring sites show very different trends of ammonium balance versus total inorganic mass concentration (Fig. S11). For CSN, the ammonium balance decreases with mass concentration whereas CASTNET remains nearly constant. This is similar to the comparison between SAGA and AMS in Fig. 4. This difference between the two sampling techniques may be due to the lack of denuder in CASTNET to remove gas-phase ammonia. The use of the denuders has led to CSN and other monitoring networks that use denuders to be more in-line with in-situ observations (Kim et al., 2015; Weber et al., 2016). Further, as shown in Fig. S8, exposure of an unprotected acidic filter for time greater than 1 day will lead to ammonia reacting with the acid to form ammonium bisulfate or ammonium sulfate, even at low ammonia mixing ratios. Other aspects that could impact this comparison, and are beyond the scope of this study (but has been discussed in other studies (Hering and Cass, 1999; Schauer et al., 2003; Chow et al., 2005, 2010; Dzepina et al., 2007; Watson et al., 2009; Nie et al., 2010; Liu et al., 2014, 2015; Cheng and He, 2015; Heim et al., 2020)), include the loss of volatile ammonium from the evaporation of ammonium nitrate or differences in the handling, shipping, and/or storage of the filters or extracted samples. Thus, without denuders, or handling of filters with more than one person present, will lead to similar differences between in-situ sampling versus filter collection of inorganic aerosols observed during various aircraft campaigns.

643 Further, the uptake of ammonia onto acidic aerosols will impact comparisons with  
644 chemical transport models (CTMs) and the understanding of various physical processes. For  
645 example, various CTMs predict different results for the mass concentration of ammonium in the  
646 upper troposphere (Wang et al., 2008a; Fisher et al., 2011; Ge et al., 2018), and selection of one  
647 measurement versus the other will lead to different degrees of agreement. For example, for filters  
648 that collect aerosols similar to those described here (no ammonia scrubber and/or exposed to  
649 human emissions of ammonia), values of ammonium  $< 0.2 \mu\text{g sm}^{-3}$  should be used with caution  
650 or instead use *on-line* measurements of ammonium (specifically for SAGA measurements but a  
651 similar analysis should be conducted for other filter-based measurements). This different  
652 agreement impacts our understanding of important processes, such as the direct radiative impact  
653 of inorganic aerosol (Wang et al., 2008b) or deposition of inorganic gases and aerosols (Nenes et  
654 al., 2020a), as the gas-phase species have a faster deposition rate than the aerosol-phase. Finally,  
655 the measurement biases can impact the suggested regulations to improve air quality (Nenes et al.,  
656 2020b) and the calculated aerosol pH, as the pH is sensitive to the partitioning of ammonia  
657 between the aerosol- and gas-phase (e.g., Hennigan et al., 2015).

658

## 659 **Conclusions**

660 Collection of aerosols onto filters to measure aerosol mass concentration and composition  
661 is valuable for improving our understanding of the emissions and chemistry of inorganic aerosol,  
662 and longstanding, multi-decadal filter-based records of atmospheric composition are invaluable  
663 to analyze atmospheric change. However, as had been discussed in earlier studies, acidic aerosols  
664 collected on filters are susceptible to uptake of gas-phase ammonia, which interacts with the

665 acidic aerosol to form an ammonium salt (e.g., ammonium bisulfate or ammonium sulfate). This  
666 artifact in filter measurements can bias our understanding on the chemical composition of the  
667 aerosol, which impacts numerous atmospheric processes.

668       We show that across six different aircraft campaigns, the aerosol collected on filters  
669 showed a substantially higher ammonium mass concentration and ammonium balance compared  
670 to AMS measurements. Further, another *on-line* measurement (PALMS) also shows lower  
671 ammonium-to-sulfate ratios than for the filters. These differences are not due to differences in  
672 the aerosol size ranges sampled by the PALMS and the filters. Instead, we show that the mixing  
673 ratio of gas-phase ammonia in the cabin of the DC-8 is high enough (mean  $\sim 45$  ppbv), and  
674 similar to other indoor environments, to interact with acidic aerosol collected on filters in  $\leq 10$  s,  
675 to form ammonium salts. These results are consistent with prior studies investigating this  
676 interference. Thus, due to the interaction of ammonia in the cabin of research aircraft, we suggest  
677 that a more realistic limit-of-detection of ammonium for the SAGA filters is  $200 \text{ ng sm}^{-3}$ , versus  
678 the  $10 \text{ ng sm}^{-3}$  typically cited based on the ion chromatography measurement. Finally, even  
679 though methods to reduce this bias have been implemented in several ground-based long-term  
680 filter measurements of inorganic aerosols, there are still some networks that collect inorganic  
681 aerosol without denuders to remove gas-phase ammonia, leading to similar discrepancies  
682 between ground networks as observed between filters and AMS on the various aircraft  
683 campaigns. Careful practice in both the aerosol collection and filtering handling is necessary to  
684 better understand the emissions, chemistry, and chemical and physical properties of inorganic  
685 aerosol.

686  
687

## 688 Acknowledgements

689

690 This study was supported by NASA grants NNX15AH33A, NNX15AJ23G, 80NSSC18K0630,  
691 and 80NSSC19K0124. We thank Glenn Diskin and the DACOM team for the use of the CO<sub>2</sub>  
692 measurements from FIREX-AQ, Armin Wisthaler for the use of the NH<sub>3</sub> measurements from  
693 FIREX-AQ, Paul Wennberg for the use of HCN measurements from FIREX-AQ, Bruce  
694 Anderson, Luke Ziemba, and the LARGE team for the use of the LAS volume distribution from  
695 SEAC<sup>4</sup>RS, Karl Froyd, Gregory Schill, and Daniel Murphy for the use of the PALMS  
696 observations from ATom-1 and -2, and Charles Brock, Agnieszka Kupc, and Christina  
697 Williamson for the volume distribution measurements during ATom-1 and -2. Also, we thank J.  
698 Andrew Neuman for the use of the Picarro G2103 during FIREX-AQ. We thank the crew of the  
699 DC-8 and C-130 aircraft for extensive support in the field deployments. We specifically thank  
700 Adam Webster and the crew of the NASA DC-8 in their assistance and persistence in allowing us  
701 to install the Picarro G2103 during FIREX-AQ in order to measure ammonia in the cabin.

702

## 703 Data Availability

704

705 ARCTAS-A and -B measurements are available at  
706 <http://doi.org/10.5067/SUBORBITAL/ARCTAS2008/DATA001>, last access 27 April 2020.  
707 SEAC<sup>4</sup>RS measurements are available at  
708 <http://doi.org/10.5067/Aircraft/SEAC4RS/Aerosol-TraceGas-Cloud>, last access 27 April 2020.  
709 WINTER measurements are available at [https://data.eol.ucar.edu/master\\_lists/generated/winter/](https://data.eol.ucar.edu/master_lists/generated/winter/),  
710 last access 27 April 2020. ATom-1 and -2 measurements are available at  
711 <https://doi.org/10.3334/ORNLDAAAC/1581>, last access 27 April 2020. Ammonia and carbon  
712 dioxide measurements from the cabin of the DC-8 are available as an attachment . CSN and  
713 CASTNET measurements are available at  
714 <http://views.cira.colostate.edu/fed/QueryWizard/Default.aspx>, last access 27 April 2020. Figures  
715 are available at [http://cires1.colorado.edu/jimenez/group\\_pubs.html](http://cires1.colorado.edu/jimenez/group_pubs.html).

716

## 717 Competing Interests

718 The authors declare no competing interests.

719

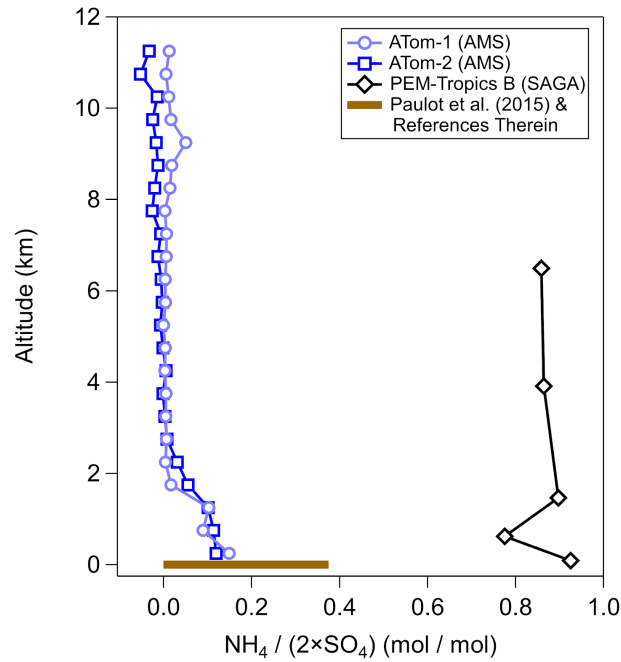
## 720 Author Contribution

721 B.A.N., P.C.-J., D.A.D., and J.L.J. designed the experiment and wrote the paper. B.A.N., P.C.-J.,  
722 D.A.D., H.G., A.V.H., D.P., J.C.S., M.K.S., M.J.C., J.E.D., W.H., and B.B.P. collected and  
723 analyzed the data. D.S.J. and A.H. ran GEOS-Chem and provided the output. All authors  
724 reviewed the paper.



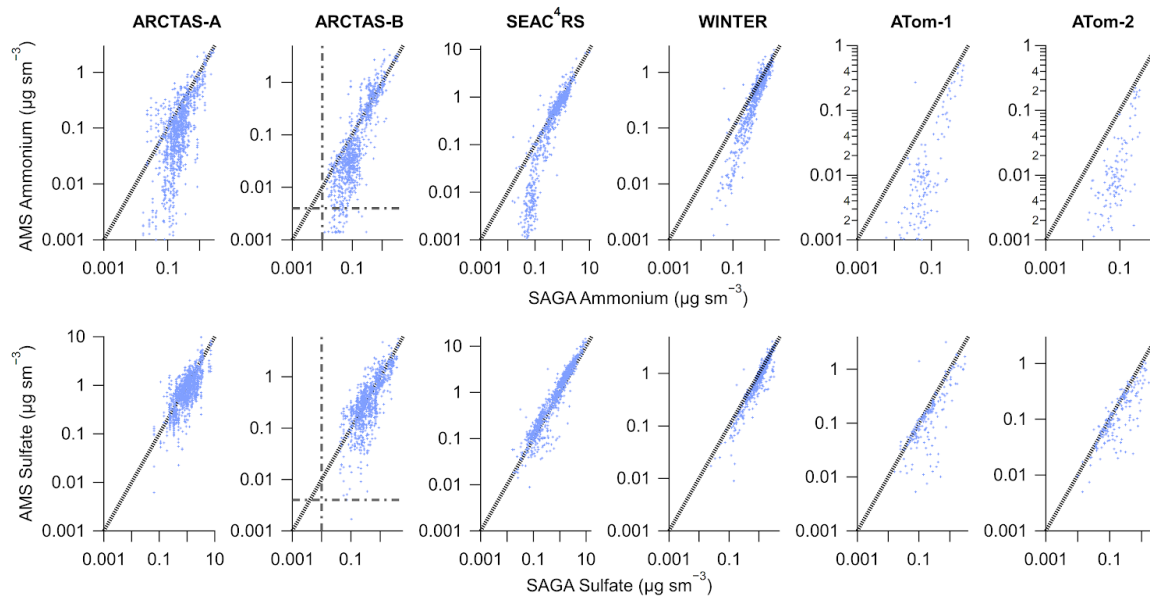
725 **Figures**

726

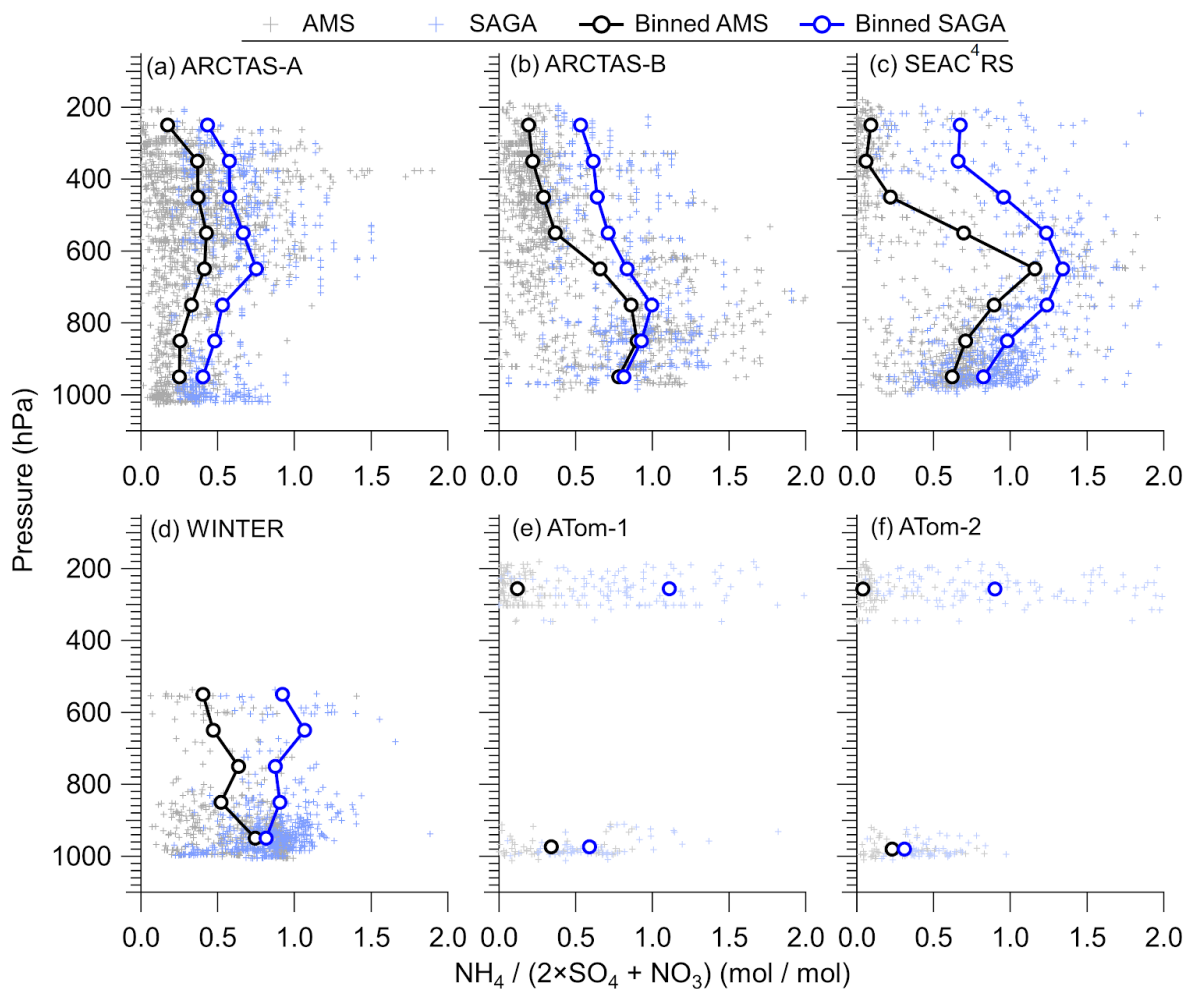


727 Figure 1. Vertical profile of sulfate-only ion molar balance ( $\text{moles}(\text{NH}_4)/\text{moles}(\text{SO}_4)$ ) measured  
728 during PEM-Tropics by collecting the aerosol on filters and analyzing it off-line with ion  
729 chromatography (Dibb et al., 2002) and during ATom-1 and -2 by AMS (Hodzic et al., 2020).  
730 The ammonium balance profile is for observations collected during ATom-1 and -2 between  
731  $-20^\circ\text{S}$  and  $20^\circ\text{N}$  in the Pacific basin, so that the observations were in a similar location as the  
732 PEM-Tropics samples. Also shown is the ammonium balance from observations summarized in  
733 Paulot et al. (2015), and reference therein, for the area around the same location as  
734 PEM-Tropics.

735



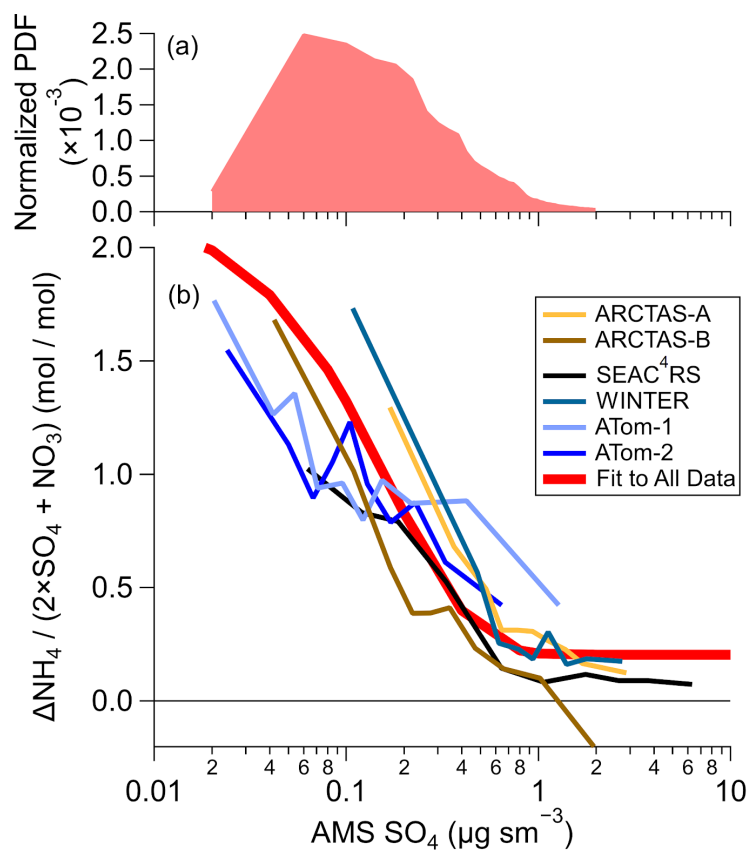
737 Figure 2. Scatter plot of AMS (y-axis) versus SAGA filter (x-axis) ammonium (top) and sulfate  
 738 (bottom) mass concentration from 6 different aircraft campaigns. AMS data have been averaged  
 739 over the SAGA filter collection times. Black line is the one-to-one line and the grey dash-dot  
 740 lines are the estimated detection limits for AMS (DeCarlo et al., 2006; Guo et al., 2020) at the  
 741 SAGA filter collection interval (~5 minutes) and the estimated detection limits for SAGA (Dibb et  
 742 al., 1999). Data has been averaged to the sampling time of SAGA and has not been filtered for  
 743 supermicron particles. For ATom-1 and -2, data during ascent and descent has been removed  
 744 (only level sampling at low altitude and high altitude).



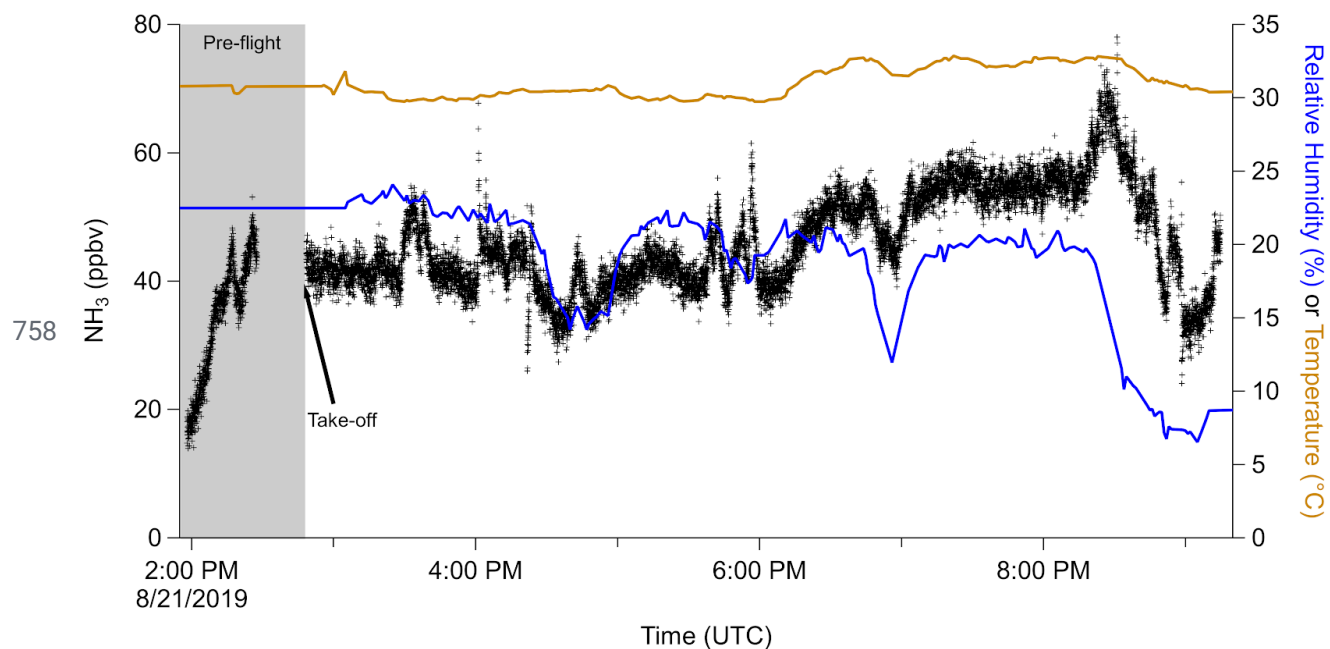
746 Figure 3. Vertical profiles of ammonium balance  $((\text{NH}_4/18)/(2 \times \text{SO}_4/96 + \text{NO}_3/62))$  for (a)  
 747 ARCTAS-A, (b) ARCTAS-B, (c) SEAC<sup>4</sup>RS, (d) WINTER, (e) ATom-1, and (f) ATom-2, for AMS  
 748 and SAGA. The binned data is the mean for each 100 hPa pressure level. The data has been  
 749 averaged to the sampling time of SAGA filters.

750

751



752 Figure 4. (a) Predicted normalized probability distribution function (PDF) for tropospheric  
 753 (pressure > 250 hPa) sulfate from GEOS-Chem for one model year (see SI). (b) Difference  
 754 between SAGA and AMS ammonium, in  $\text{mol sm}^{-3}$ , divided by AMS sulfate and nitrate, in  $\text{mol}$   
 755  $\text{sm}^{-3}$ , versus AMS sulfate ( $\mu\text{g sm}^{-3}$ ), for the six different airborne campaigns. The values shown  
 756 are binned deciles for the five different airborne campaigns. The fit shown in (b) is for all data  
 757 from all campaigns.



759 Figure 5. Time series of ammonia (left) and relative humidity and temperature (right) measured  
 760 inside the cabin of the NASA DC-8 during a flight during the FIREX-AQ campaign. Time spent  
 761 prior to take-off is marked with a grey background.

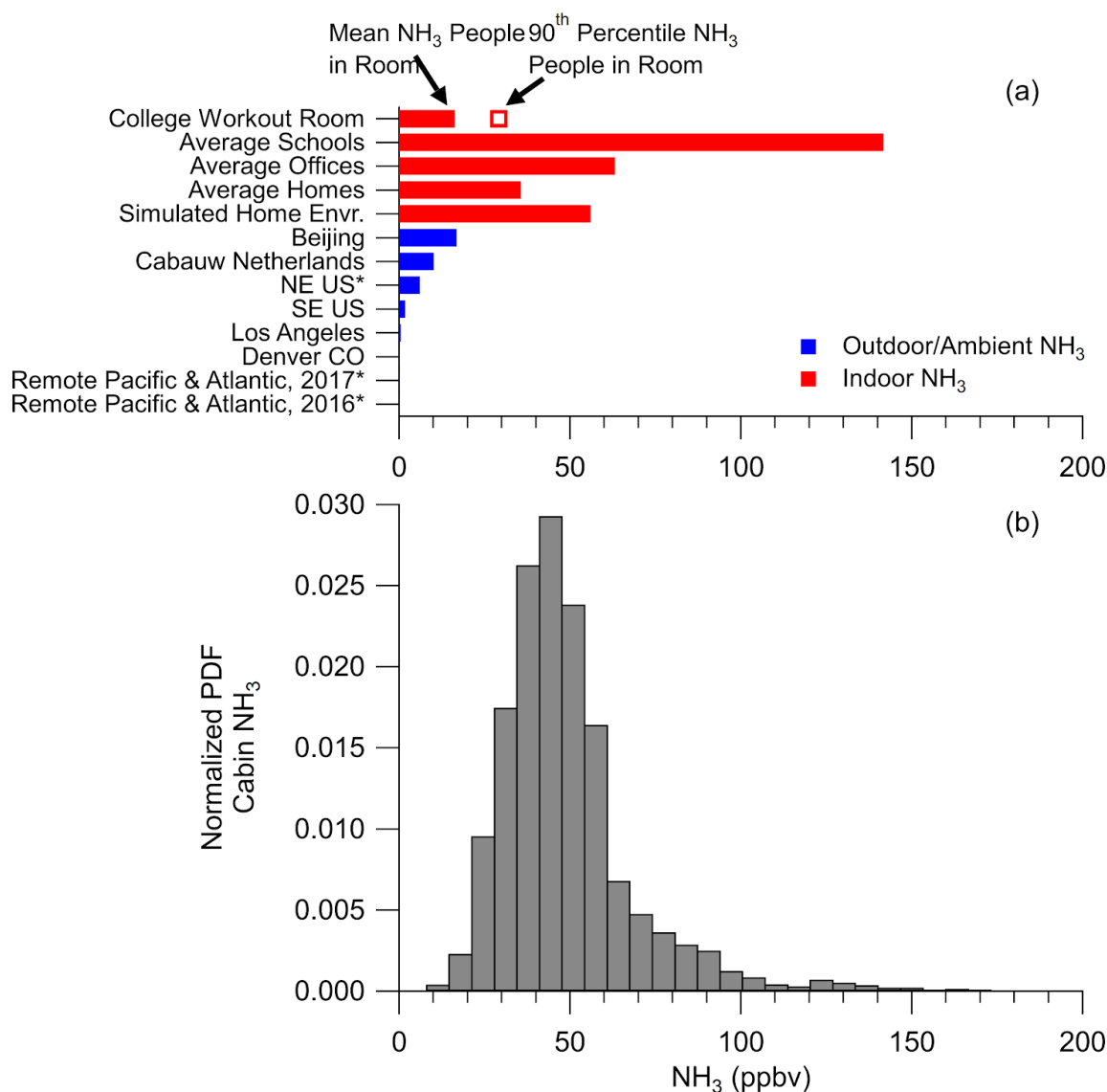


Figure 6. (a) Ammonia ( $\text{NH}_3$ ) (ppbv) reported for studies. See Table S1 for references. Asterisk after study name indicates  $\text{NH}_3$  predicted by thermodynamic model instead of being measured. (b) Normalized probability distribution function (PDF) for  $\text{NH}_3$ , measured in the cabin of the NASA DC-8 during FIREX-AQ.

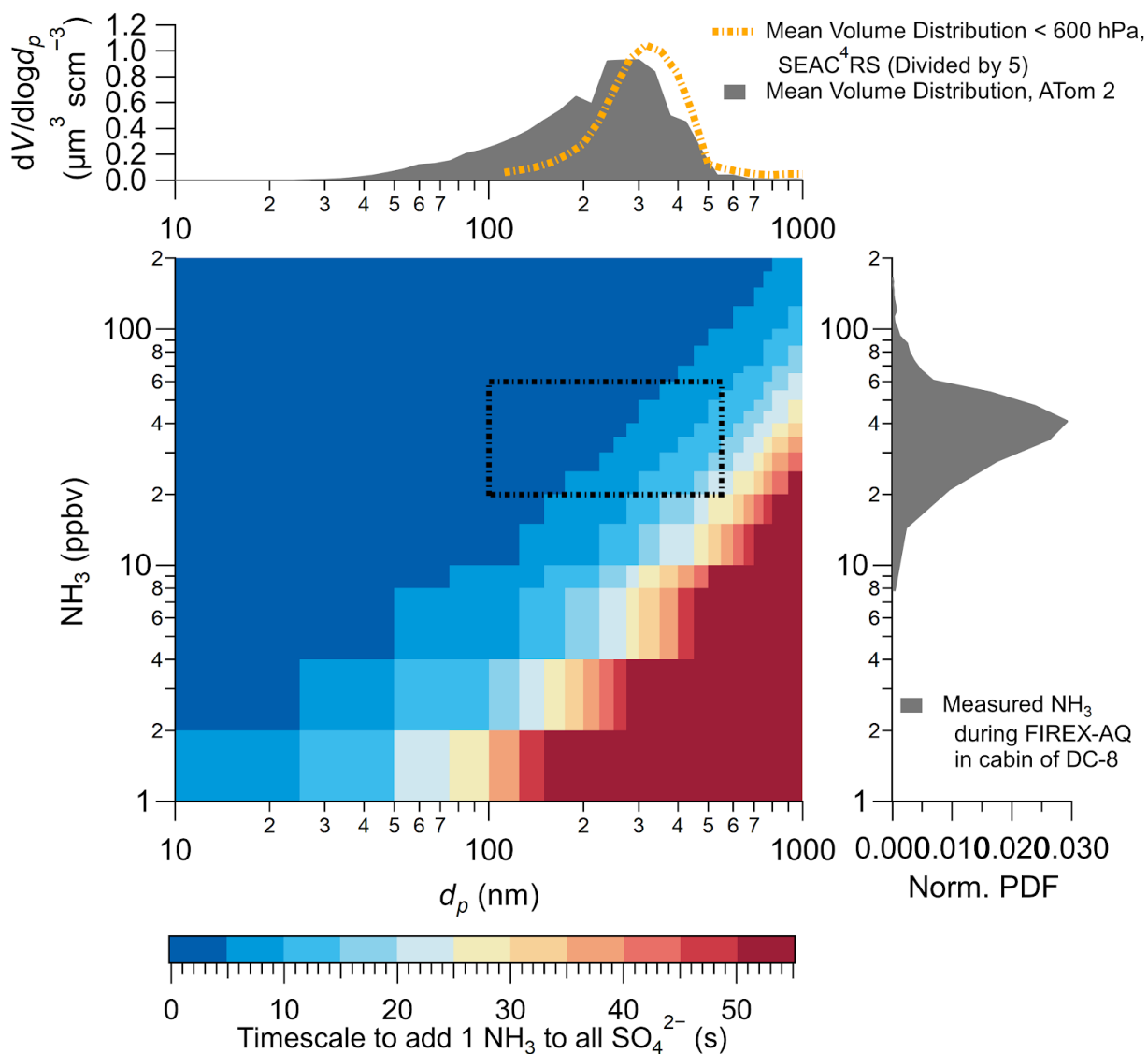


Figure 7. Theoretical calculation for the amount of time it would take for all the sulfuric acid on the filter to react with one ammonia molecule to become ammonium bisulfate. Volume distribution is the average from SEAC<sup>4</sup>RS and ATom-2 (adapted from Guo et al. (2020)) and the normalized probability distribution function (Norm. PDF) is from Fig. 6. The representative diameter and ammonia mixing ratio are shown as dashed lines in the calculated timescale.

## 773 References

- 774 Abbatt, J. P. D., Benz, S., Cziczo, D. J., Kanji, Z., Lohmann, U. and Möhler, O.: Solid  
775 ammonium sulfate aerosols as ice nuclei: a pathway for cirrus cloud formation, *Science*,  
776 313(5794), 1770–1773, 2006.
- 777 Aknan, A.: NASA Airborne Science Data for Atmospheric Composition, TABMEP2  
778 POLARCAT Preliminary Assessment Reports [online] Available from:  
779 <http://www-air.larc.nasa.gov/> (Accessed 3 June 2020), 2015.
- 780 Ampollini, L., Katz, E. F., Bourne, S., Tian, Y., Novoselac, A., Goldstein, A. H., Lucic, G.,  
781 Waring, M. S. and DeCarlo, P. F.: Observations and Contributions of Real-Time Indoor  
782 Ammonia Concentrations during HOMEChem, *Environ. Sci. Technol.*, 53(15), 8591–8598,  
783 2019.
- 784 Bahreini, R., Dunlea, E. J., Matthew, B. M., Simons, C., Docherty, K. S., DeCarlo, P. F., Jimenez,  
785 J. L., Brock, C. A. and Middlebrook, A. M.: Design and Operation of a Pressure-Controlled Inlet  
786 for Airborne Sampling with an Aerodynamic Aerosol Lens, *Aerosol Sci. Technol.*, 42(6),  
787 465–471, 2008.
- 788 Bahreini, R., Ervens, B., Middlebrook, A. M., Warneke, C., De Gouw, J. A., DeCarlo, P. F.,  
789 Jimenez, J. L., Brock, C. A., Neuman, J. A., Ryerson, T. B., Stark, H., Atlas, E., Brioude, J.,  
790 Fried, A., Holloway, J. S., Peischl, J., Richter, D., Walega, J., Weibring, P., Wollny, A. G. and  
791 Fehsenfeld, F. C.: Organic aerosol formation in urban and industrial plumes near Houston and  
792 Dallas, Texas, *J. Geophys. Res. D: Atmos.*, 114(16), 1–17, 2009.
- 793 Baltensperger, U., Barrie, L., Frohlich, C., Gras, J., Jäger, H., Jennings, S. G., Li, S.-M., Ogren,  
794 J., Widensohler, A., Wehrli, C. and Wilson, J.: WMO/GAW Aerosol Measurement Procedures  
795 Guidelines and Recommendations, WMO GAW. [online] Available from:  
796 [https://library.wmo.int/doc\\_num.php?explnum\\_id=9244](https://library.wmo.int/doc_num.php?explnum_id=9244), 2003.
- 797 von Bobritzki, K., Braban, C. F., Famulari, D., Jones, S. K., Blackall, T., Smith, T. E. L., Blom,  
798 M., Coe, H., Gallagher, M., Ghalaieny, M., McGillen, M. R., Percival, C. J., Whitehead, J. D.,  
799 Ellis, R., Murphy, J., Mohacsi, A., Pogany, A., Junninen, H., Rantanen, S., Sutton, M. A. and  
800 Nemitz, E.: Field inter-comparison of eleven atmospheric ammonia measurement techniques,  
801 *Atmos. Meas. Tech.*, 3(1), 91–112, 2010.
- 802 Brock, C. A., Williamson, C., Kupc, A., Froyd, K. D., Erdesz, F., Wagner, N., Richardson, M.,  
803 Schwarz, J. P., Gao, R.-S., Katich, J. M., Campuzano-Jost, P., Nault, B. A., Schroder, J. C.,  
804 Jimenez, J. L., Weinzierl, B., Dollner, M., Bui, T. and Murphy, D. M.: Aerosol size distributions  
805 during the Atmospheric Tomography Mission (ATom): methods, uncertainties, and data products,  
806 *Atmos. Meas. Tech.*, 12(6), 3081–3099, 2019.
- 807 Brundrett, G.: Comfort and health in commercial aircraft: a literature review, *J. R. Soc. Promot.*  
808 *Health*, 121(1), 29–37, 2001.
- 809 Canagaratna, M. R., Jayne, J. T., Jimenez, J. L., Allan, J. D., Alfarra, M. R., Zhang, Q., Onasch,



810 T. B., Drewnick, F., Coe, H., Middlebrook, A., Delia, A., Williams, L. R., Trimborn, A. M.,  
811 Northway, M. J., DeCarlo, P. F., Kolb, C. E., Davidovits, P. and Worsnop, D. R.: Chemical and  
812 microphysical characterization of ambient aerosols with the aerodyne aerosol mass spectrometer,  
813 *Mass Spectrom. Rev.*, 26(2), 185–222, 2007.

814 Cheng, Y. and He, K.-B.: Measurement of carbonaceous aerosol with different sampling  
815 configurations and frequencies, *Atmos. Meas. Tech.*, 8(7), 2639–2648, 2015.

816 Chow, J. C., Watson, J. G., Lowenthal, D. H. and Magliano, K. L.: Loss of PM<sub>2.5</sub> Nitrate from  
817 Filter Samples in Central California, *J. Air Waste Manage. Assoc.*, 55(8), 1158–1168, 2005.

818 Chow, J. C., Watson, J. G., Chen, L.-W. A., Rice, J. and Frank, N. H.: Quantification of PM<sub>2.5</sub>  
819 organic carbon sampling artifacts in US networks, *Atmos. Chem. Phys.*, 10(12), 5223–5239,  
820 2010.

821 Clark, K. W., Anderson, K. R., Linn, W. S. and Gong, H., Jr: Influence of breathing-zone  
822 ammonia on human exposures to acid aerosol pollution, *J. Air Waste Manag. Assoc.*, 45(11),  
823 923–925, 1995.

824 Cohen, A. J., Brauer, M., Burnett, R., Anderson, H. R., Frostad, J., Estep, K., Balakrishnan, K.,  
825 Brunekreef, B., Dandona, L., Dandona, R., Feigin, V., Freedman, G., Hubbell, B., Jobling, A.,  
826 Kan, H., Knibbs, L., Liu, Y., Martin, R., Morawska, L., Pope, C. A., Shin, H., Straif, K.,  
827 Shaddick, G., Thomas, M., van Dingenen, R., van Donkelaar, A., Vos, T., Murray, C. J. L. and  
828 Forouzanfar, M. H.: Estimates and 25-year trends of the global burden of disease attributable to  
829 ambient air pollution: an analysis of data from the Global Burden of Diseases Study 2015,  
830 *Lancet*, 389(10082), 1907–1918, 2017.

831 Colberg, C. A., Luo, B. P., Wernli, H., Koop, T. and Peter, T.: A novel model to predict the  
832 physical state of atmospheric H<sub>2</sub>SO<sub>4</sub>/NH<sub>3</sub>/H<sub>2</sub>O aerosol particles, *Atmos. Chem. Phys.*, 3(4),  
833 909–924, 2003.

834 Coury, C. and Dillner, A. M.: ATR-FTIR characterization of organic functional groups and  
835 inorganic ions in ambient aerosols at a rural site, *Atmos. Environ.*, 43(4), 940–948, 2009.

836 Cozic, J., Verheggen, B., Weingartner, E., Crosier, J., Bower, K. N., Flynn, M., Coe, H.,  
837 Henning, S., Steinbacher, M., Henne, S., Collaud Coen, M., Petzold, A. and Baltensperger, U.:  
838 Chemical composition of free tropospheric aerosol for PM<sub>1</sub> and coarse mode at the high alpine  
839 site Jungfraujoch, *Atmos. Chem. Phys.*, 8(2), 407–423, 2008.

840 Cubison, M. J., Ortega, A. M., Hayes, P. L., Farmer, D. K., Day, D. A., Lechner, M. J., Brune, W.  
841 H., Apel, E., Diskin, G. S., Fisher, J. A., Fuelberg, H. E., Hecobian, A., Knapp, D. J., Mikoviny,  
842 T., Riemer, D., Sachse, G. W., Sessions, W., Weber, R. J., Weinheimer, A. J., Wisthaler, A. and  
843 Jimenez, J. L.: Effects of aging on organic aerosol from open biomass burning smoke in aircraft  
844 and laboratory studies, *Atmos. Chem. Phys.*, 11(23), 12049–12064, 2011.

845 Daumer, B., Niessner, R. and Klockow, D.: Laboratory studies of the influence of thin organic  
846 films on the neutralization reaction of H<sub>2</sub>SO<sub>4</sub> aerosol with ammonia, *J. Aerosol Sci.*, 23(4),

847 315–325, 1992.

848 DeCarlo, P. F., Kimmel, J. R., Trimborn, A., Northway, M. J., Jayne, J. T., Aiken, A. C., Gonin,  
849 M., Fuhrer, K., Horvath, T., Docherty, K. S., Worsnop, D. R. and Jimenez, J. L.:  
850 Field-deployable, high-resolution, time-of-flight aerosol mass spectrometer, *Anal. Chem.*,  
851 78(24), 8281–8289, 2006.

852 DeCarlo, P. F., Dunlea, E. J., Kimmel, J. R., Aiken, A. C., Sueper, D., Crounse, J., Wennberg, P.  
853 O., Emmons, L., Shinozuka, Y., Clarke, A., Zhou, J., Tomlinson, J., Collins, D. R., Knapp, D.,  
854 Weinheimer, A. J., Montzka, D. D., Campos, T. and Jimenez, J. L.: Fast airborne aerosol size and  
855 chemistry measurements above Mexico City and Central Mexico during the MILAGRO  
856 campaign, *Atmos. Chem. Phys.*, 8(14), 4027–4048, 2008.

857 Dentener, F. J. and Crutzen, P. J.: A three-dimensional model of the global ammonia cycle, *J.*  
858 *Atmos. Chem.*, 19(4), 331–369, 1994.

859 Dibb, J. E., Talbot, R. W., Scheuer, E. M., Blake, D. R., Blake, N. J., Gregory, G. L., Sachse, G.  
860 W. and Thornton, D. C.: Aerosol chemical composition and distribution during the Pacific  
861 Exploratory Mission (PEM) Tropics, *J. Geophys. Res.*, 104(D5), 5785–5800, 1999.

862 Dibb, J. E., Talbot, R. W. and Scheuer, E. M.: Composition and distribution of aerosols over the  
863 North Atlantic during the Subsonic Assessment Ozone and Nitrogen Oxide Experiment  
864 (SONEX), *J. Geophys. Res. D: Atmos.*, 105(D3), 3709–3717, 2000.

865 Dibb, J. E., Talbot, R. W., Seid, G., Jordan, C., Scheuer, E., Atlas, E., Blake, N. J. and Blake, D.  
866 R.: Airborne sampling of aerosol particles: Comparison between surface sampling at Christmas  
867 Island and P-3 sampling during PEM-Tropics B, *J. Geophys. Res.*, 108(D2), 11335, 2002.

868 Dibb, J. E., Talbot, R. W., Scheuer, E. M., Seid, G., Avery, M. A. and Singh, H. B.: Aerosol  
869 chemical composition in Asian continental outflow during the TRACE-P campaign: Comparison  
870 with PEM-West B, *J. Geophys. Res.: Atmos.*, 108(D21), 8815, 2003.

871 Dzepina, K., Arey, J., Marr, L. C., Worsnop, D. R., Salcedo, D., Zhang, Q., Onasch, T. B.,  
872 Molina, L. T., Molina, M. J. and Jimenez, J. L.: Detection of particle-phase polycyclic aromatic  
873 hydrocarbons in Mexico City using an aerosol mass spectrometer, *Int. J. Mass Spectrom.*, 263(2),  
874 152–170, 2007.

875 Faloona, I.: Sulfur processing in the marine atmospheric boundary layer: A review and critical  
876 assessment of modeling uncertainties, *Atmos. Environ.*, 43(18), 2841–2854, 2009.

877 Filges, A., Gerbig, C., Rella, C. W., Hoffnagle, J., Smit, H., Krämer, M., Spelten, N., Rolf, C.,  
878 Bozóki, Z., Buchholz, B. and Ebert, V.: Evaluation of the IAGOS-Core GHG package H<sub>2</sub>O  
879 measurements during the DENCHAR airborne inter-comparison campaign in 2011, *Atmos.*  
880 *Meas. Tech.*, 11(9), 5279–5297, 2018.

881 Finewax, Z., Pagonis, D., Claflin, M. S., Handschy, A. V., Brown, W. L., Ba, J. O. N., Lerner, B.  
882 M., Jimenez, J. L., Ziemann, P. J. and de Gouw, J. A.: Quantification and source characterization

883 of volatile organic compounds from exercising and application of chlorine-based cleaning  
884 products in a university athletic center, *Indoor Air*, Submitted, 2020.

885 Fisher, J. A., Jacob, D. J., Wang, Q., Bahreini, R., Carouge, C. C., Cubison, M. J., Dibb, J. E.,  
886 Diehl, T., Jimenez, J. L., Leibensperger, E. M., Lu, Z., Meinders, M. B. J., Pye, H. O. T., Quinn,  
887 P. K., Sharma, S., Streets, D. G., van Donkelaar, A. and Yantosca, R. M.: Sources, distribution,  
888 and acidity of sulfate–ammonium aerosol in the Arctic in winter–spring, *Atmos. Environ.*,  
889 45(39), 7301–7318, 2011.

890 Freney, E., Sellegri Karine, S. K., Eija, A., Clemence, R., Aurelien, C., Jean-Luc, B., Aurelie, C.,  
891 Hervo Maxime, H. M., Nadege, M., Laetitia, B. and David, P.: Experimental Evidence of the  
892 Feeding of the Free Troposphere with Aerosol Particles from the Mixing Layer, *Aerosol Air*  
893 *Qual. Res.*, 16(3), 702–716, 2016.

894 Fröhlich, R., Cubison, M. J., Slowik, J. G., Bukowiecki, N., Canonaco, F., Croteau, P. L., Gysel,  
895 M., Henne, S., Herrmann, E., Jayne, J. T., Steinbacher, M., Worsnop, D. R., Baltensperger, U.  
896 and Prévôt, A. S. H.: Fourteen months of on-line measurements of the non-refractory submicron  
897 aerosol at the Jungfraujoch (3580 m a.s.l.) – chemical composition, origins and organic aerosol  
898 sources, *Atmos. Chem. Phys.*, 15(19), 11373–11398, 2015.

899 Froyd, K. D., Murphy, D. M., Sanford, T. J., Thomson, D. S., Wilson, J. C., Pfister, L. and Lait,  
900 L.: Aerosol composition of the tropical upper troposphere, *Atmos. Chem. Phys.*, 9(13),  
901 4363–4385, 2009.

902 Froyd, K. D., Murphy, D. M., Brock, C. A., Campuzano-Jost, P., Dibb, J. E., Jimenez, J.-L.,  
903 Kupc, A., Middlebrook, A. M., Schill, G. P., Thornhill, K. L., Williamson, C. J., Wilson, J. C.  
904 and Ziemba, L. D.: A new method to quantify mineral dust and other aerosol species from  
905 aircraft platforms using single-particle mass spectrometry, *Atmos. Meas. Tech.*, 12(11),  
906 6209–6239, 2019.

907 Fuchs, N. A. and Sutugin, A. G.: High-Dispersed Aerosols, in *Topics in Current Aerosol*  
908 *Research*, edited by G. M. Hidy and J. R. Brock, Pergamon., 1971.

909 Ge, C., Zhu, C., Francisco, J. S., Zeng, X. C. and Wang, J.: A molecular perspective for global  
910 modeling of upper atmospheric NH<sub>3</sub> from freezing clouds, *Proc. Natl. Acad. Sci. U. S. A.*,  
911 115(24), 6147–6152, 2018.

912 Guo, H., Xu, L., Bougiatioti, A., Cerully, K. M., Capps, S. L., Hite, J. R., Carlton, A. G., Lee,  
913 S.-H., Bergin, M. H., Ng, N. L., Nenes, A. and Weber, R. J.: Fine-particle water and pH in the  
914 southeastern United States, *Atmos. Chem. Phys.*, 15(9), 5211–5228, 2015.

915 Guo, H., Sullivan, A. P., Campuzano-Jost, P., Schroder, J. C., Lopez-Hilfiker, F. D., Dibb, J. E.,  
916 Jimenez, J. L., Thornton, J. A., Brown, S. S., Nenes, A. and Weber, R. J.: Fine particle pH and  
917 the partitioning of nitric acid during winter in the northeastern United States, *J. Geophys. Res. D:*  
918 *Atmos.*, 121(17), 10,355–10,376, 2016.

919 Guo, H., Nenes, A. and Weber, R. J.: The underappreciated role of nonvolatile cations in aerosol

920 ammonium-sulfate molar ratios, *Atmos. Chem. Phys.*, 18(23), 17307–17323, 2018.

921 Guo, H., Campuzano-Jost, P., Nault, B. A., Day, D. A., Schroder, J. C., Dibb, J. E., Dollner, M.,  
 922 Weinzierl, B. and Jimenez, J. L.: The Importance of Size Ranges in Intercomparison of Aerosol  
 923 Volume Concentration Measurements: A Case Study for Aerosol Mass Spectrometer in the  
 924 ATom Mission, *Atmos. Meas. Tech. Discuss.*, In Review, doi:10.5194/amt-2020-224, 2020.

925 Hanson, D. and Kosciuch, E.: The  $\text{NH}_3$  Mass Accommodation Coefficient for Uptake onto  
 926 Sulfuric Acid Solutions, *J. Phys. Chem. A*, 107(13), 2199–2208, 2003.

927 Hanson, D. R. and Kosciuch, E.: Reply to “Comment on ‘The  $\text{NH}_3$  Mass Accommodation  
 928 Coefficient for Uptake onto Sulfuric Acid Solutions,’” *J. Phys. Chem. A*, 108(40), 8549–8551,  
 929 2004.

930 Hayes, D., Snetsinger, K., Ferry, G., Oberbeck, V. and Farlow, N.: Reactivity of stratospheric  
 931 aerosols to small amounts of ammonia in the laboratory environment, *Geophys. Res. Lett.*, 7(11),  
 932 974–976, 1980.

933 Heald, C. L. and Kroll, J. H.: The fuel of atmospheric chemistry: Toward a complete description  
 934 of reactive organic carbon, *Sci Adv*, 6(6), eaay8967, 2020.

935 Heald, C. L., Collett, J. L., Jr., Lee, T., Benedict, K. B., Schwandner, F. M., Li, Y., Clarisse, L.,  
 936 Hurtmans, D. R., Van Damme, M., Clerbaux, C., Coheur, P.-F., Philip, S., Martin, R. V. and Pye,  
 937 H. O. T.: Atmospheric ammonia and particulate inorganic nitrogen over the United States,  
 938 *Atmos. Chem. Phys.*, 12(21), 10295–10312, 2012.

939 Heim, E. W., Dibb, J., Scheuer, E., Jost, P. C., Nault, B. A., Jimenez, J. L., Peterson, D., Knote,  
 940 C., Fenn, M., Hair, J., Beyersdorf, A. J., Corr, C. and Anderson, B. E.: Asian dust observed  
 941 during KORUS-AQ facilitates the uptake and incorporation of soluble pollutants during transport  
 942 to South Korea, *Atmos. Environ.*, 224, 117305, 2020.

943 Hennigan, C. J., Sullivan, A. P., Fountoukis, C. I., Nenes, A., Hecobian, A., Vargas, O., Peltier,  
 944 R. E., Hanks, A. T. C., Huey, L. G., Lefer, B. L., Russell, A. G. and Weber, R. J.: On the  
 945 volatility and production mechanisms of newly formed nitrate and water soluble organic aerosol  
 946 in Mexico City, *Atmos. Chem. Phys.*, 8(14), 3761–3768, 2008.

947 Hennigan, C. J., Izumi, J., Sullivan, A. P., Weber, R. J. and Nenes, A.: A critical evaluation of  
 948 proxy methods used to estimate the acidity of atmospheric particles, *Atmos. Chem. Phys.*, 15(5),  
 949 2775–2790, 2015.

950 Henze, D. K., Seinfeld, J. H. and Shindell, D. T.: Inverse modeling and mapping US air quality  
 951 influences of inorganic  $\text{PM}_{2.5}$  precursor emissions using the adjoint of GEOS-Chem, *Atmos.*  
 952 *Chem. Phys.*, 9(16), 5877–5903, 2009.

953 Hering, S. and Cass, G.: The Magnitude of Bias in the Measurement of  $\text{PM}_{25}$  Arising from  
 954 Volatilization of Particulate Nitrate from Teflon Filters, *J. Air Waste Manag. Assoc.*, 49(6),

955 725–733, 1999.

956 Hocking, M. B.: Indoor air quality: recommendations relevant to aircraft passenger cabins, *Am.*  
957 *Ind. Hyg. Assoc. J.*, 59(7), 446–454, 1998.

958 Hodzic, A. and Duvel, J. P.: Impact of Biomass Burning Aerosols on the Diurnal Cycle of  
959 Convective Clouds and Precipitation Over a Tropical Island: Fire aerosols effect on deep  
960 convection, *J. Geophys. Res. D: Atmos.*, 123(2), 1017–1036, 2018.

961 Hodzic, A., Campuzano-Jost, P., Bian, H., Chin, M., Colarco, P. R., Day, D. A., Froyd, K. D.,  
962 Heinold, B., Jo, D. S., Katich, J. M., Kodros, J. K., Nault, B. A., Pierce, J. R., Ray, E., Schacht,  
963 J., Schill, G. P., Schroder, J. C., Schwarz, J. P., Sueper, D. T., Tegen, I., Tilmes, S., Tsigaridis, K.,  
964 Yu, P. and Jimenez, J. L.: Characterization of Organic Aerosol across the Global Remote  
965 Troposphere: A comparison of ATom measurements and global chemistry models, *Atmos.*  
966 *Chem. Phys.*, 20(8), 4607–4635, 2020.

967 Hunt, E. W. and Space, D. R.: The Airplane Cabin Environment: Issues Pertaining to Flight  
968 Attendant, in *Comfort*,” International in-flight Service Management Organization Conference.  
969 [online] Available from:  
970 <http://citeseerx.ist.psu.edu/viewdoc/similar?doi=10.1.1.304.7321&type=cc> (Accessed 25 March  
971 2020), 1994.

972 Huntzicker, J. J., Cary, R. A. and Ling, C.-S.: Neutralization of sulfuric acid aerosol by ammonia,  
973 *Environ. Sci. Technol.*, 14(7), 819–824, 1980.

974 Hu, W., Hu, M., Hu, W., Jimenez, J. L., Yuan, B., Chen, W., Wang, M., Wu, Y., Chen, C., Wang,  
975 Z., Peng, J., Zeng, L. and Shao, M.: Chemical composition, sources, and aging process of  
976 submicron aerosols in Beijing: Contrast between summer and winter, *J. Geophys. Res. D:*  
977 *Atmos.*, 121(4), 1955–1977, 2016.

978 Hu, W., Campuzano-Jost, P., Day, D. A., Croteau, P., Canagaratna, M. R., Jayne, J. T., Worsnop,  
979 D. R. and Jimenez, J. L.: Evaluation of the new capture vaporizer for aerosol mass spectrometers  
980 (AMS) through field studies of inorganic species, *Aerosol Sci. Technol.*, 51(6), 735–754, 2017a.

981 Hu, W., Campuzano-Jost, P., Day, D. A., Croteau, P., Canagaratna, M. R., Jayne, J. T., Worsnop,  
982 D. R. and Jimenez, J. L.: Evaluation of the new capture vapourizer for aerosol mass  
983 spectrometers (AMS) through laboratory studies of inorganic species, *Atmospheric Measurement*  
984 *Techniques*, 10(6), 2897–2921, 2017b.

985 Hu, W., Campuzano-Jost, P., Day, D. A., Nault, B. A., Park, T., Lee, T., Pajunoja, A., Virtanen,  
986 A., Croteau, P., Canagaratna, M. R., Jayne, J. T., Worsnop, D. R. and Jimenez, J. L.: Ambient  
987 Quantification and Size Distributions for Organic Aerosol in Aerosol Mass Spectrometers with  
988 the New Capture Vaporizer, *ACS Earth Space Chem.*, doi:10.1021/acsearthspacechem.9b00310,  
989 2020.

990 Jacob, D. J., Crawford, J. H., Maring, H., Clarke, A. D., Dibb, J. E., Emmons, L. K., Ferrare, R.  
991 A., Hostetler, C. A., Russell, P. B., Singh, H. B., Thompson, A. M., Shaw, G. E., McCauley, E.,

992 Pederson, J. R. and Fisher, J. A.: The Arctic Research of the Composition of the Troposphere  
 993 from Aircraft and Satellites (ARCTAS) mission: design, execution, and first results, *Atmos.*  
 994 *Chem. Phys.*, 10(11), 5191–5212, 2010.

995 Jimenez, J. L., Canagaratna, M. R., Donahue, N. M., Prevot, A. S. H., Zhang, Q., Kroll, J. H.,  
 996 DeCarlo, P. F., Allan, J. D., Coe, H., Ng, N. L., Aiken, A. C., Docherty, K. S., Ulbrich, I. M.,  
 997 Grieshop, A. P., Robinson, A. L., Duplissy, J., Smith, J. D., Wilson, K. R., Lanz, V. A., Hueglin,  
 998 C., Sun, Y. L., Tian, J., Laaksonen, A., Raatikainen, T., Rautiainen, J., Vaattovaara, P., Ehn, M.,  
 999 Kulmala, M., Tomlinson, J. M., Collins, D. R., Cubison, M. J., Dunlea, E. J., Huffman, J. A.,  
 1000 Onasch, T. B., Alfarra, M. R., Williams, P. I., Bower, K., Kondo, Y., Schneider, J., Drewnick, F.,  
 1001 Borrmann, S., Weimer, S., Demerjian, K., Salcedo, D., Cottrell, L., Griffin, R., Takami, A.,  
 1002 Miyoshi, T., Hatakeyama, S., Shimono, A., Sun, J. Y., Zhang, Y. M., Dzepina, K., Kimmel, J. R.,  
 1003 Sueper, D., Jayne, J. T., Herndon, S. C., Trimborn, A. M., Williams, L. R., Wood, E. C.,  
 1004 Middlebrook, A. M., Kolb, C. E., Baltensperger, U. and Worsnop, D. R.: Evolution of organic  
 1005 aerosols in the atmosphere, *Science*, 326(5959), 1525–1529, 2009.

1006 Kamp, J. N., Chowdhury, A., Adamsen, A. P. S. and Feilberg, A.: Negligible influence of  
 1007 livestock contaminants and sampling system on ammonia measurements with cavity ring-down  
 1008 spectroscopy, *Atmos. Meas. Tech.*, 12(5), 2837–2850, 2019.

1009 Kim, H., Zhang, Q. and Heo, J.: Influence of intense secondary aerosol formation and long-range  
 1010 transport on aerosol chemistry and properties in the Seoul Metropolitan Area during spring time:  
 1011 results from KORUS-AQ, *Atmos. Chem. Phys.*, 18(10), 7149–7168, 2018.

1012 Kim, P. S., Jacob, D. J., Fisher, J. A., Travis, K., Yu, K., Zhu, L., Yantosca, R. M., Sulprizio, M.  
 1013 P., Jimenez, J. L., Campuzano-Jost, P., Froyd, K. D., Liao, J., Hair, J. W., Fenn, M. A., Butler, C.  
 1014 F., Wagner, N. L., Gordon, T. D., Welti, A., Wennberg, P. O., Crounse, J. D., St Clair, J. M.,  
 1015 Teng, A. P., Millet, D. B., Schwarz, J. P., Markovic, M. Z. and Perring, A. E.: Sources,  
 1016 seasonality, and trends of southeast US aerosol: an integrated analysis of surface, aircraft, and  
 1017 satellite observations with the GEOS-Chem chemical transport model, *Atmos. Chem. Phys.*, 15,  
 1018 10411–10433, 2015.

1019 Kline, J., Huebert, B., Howell, S., Blomquist, B., Zhuang, J., Bertram, T. and Carrillo, J.: Aerosol  
 1020 composition and size versus altitude measured from the C-130 during ACE-Asia, *J. Geophys.*  
 1021 *Res.*, 109(D19), 340, 2004.

1022 Klockow, D., Jablonski, B. and Nießner, R.: Possible artifacts in filter sampling of atmospheric  
 1023 sulphuric acid and acidic sulphates, *Atmos. Environ.*, 13(12), 1665–1676, 1979.

1024 Koutrakis, P., Wolfson, J. M. and Spengler, J. D.: An improved method for measuring aerosol  
 1025 strong acidity: Results from a nine-month study in St Louis, Missouri and Kingston, Tennessee,  
 1026 *Atmos. Environ.*, 22(1), 157–162, 1988.

1027 Kupc, A., Williamson, C., Wagner, N. L., Richardson, M. and Brock, C. A.: Modification,  
 1028 calibration, and performance of the Ultra-High Sensitivity Aerosol Spectrometer for particle size  
 1029 distribution and volatility measurements during the Atmospheric Tomography Mission (ATom)



1030 airborne campaign, *Atmos. Meas. Tech.*, 11(1), 369–383, 2018.

1031 Larson, T. V., Covert, D. S., Frank, R. and Charlson, R. J.: Ammonia in the human airways:  
 1032 neutralization of inspired acid sulfate aerosols, *Science*, 197(4299), 161–163, 1977.

1033 Lavery, T. F., Rogers, C. M., Baumgardner, R. and Mishoe, K. P.: Intercomparison of Clean Air  
 1034 Status and Trends Network Nitrate and Nitric Acid Measurements with Data from Other  
 1035 Monitoring Programs, *J. Air Waste Manag. Assoc.*, 59(2), 214–226, 2009.

1036 Liao, J., Froyd, K. D., Murphy, D. M., Keutsch, F. N., Yu, G., Wennberg, P. O., St Clair, J. M.,  
 1037 Crounse, J. D., Wisthaler, A., Mikoviny, T., Jimenez, J. L., Campuzano-Jost, P., Day, D. A., Hu,  
 1038 W., Ryerson, T. B., Pollack, I. B., Peischl, J., Anderson, B. E., Ziemba, L. D., Blake, D. R.,  
 1039 Meinardi, S. and Diskin, G.: Airborne measurements of organosulfates over the continental U.S.,  
 1040 *J. Geophys. Res. D: Atmos.*, 120(7), 2990–3005, 2015.

1041 Liggio, J., Li, S.-M., Vlasenko, A., Stroud, C. and Makar, P.: Depression of ammonia uptake to  
 1042 sulfuric acid aerosols by competing uptake of ambient organic gases, *Environ. Sci. Technol.*,  
 1043 45(7), 2790–2796, 2011.

1044 Li, M., Weschler, C. J., Bekö, G., Wargocki, P., Lucic, G. and Williams, J.: Human Ammonia  
 1045 Emission Rates under Various Indoor Environmental Conditions, *Environ. Sci. Technol.*,  
 1046 doi:10.1021/acs.est.0c00094, 2020.

1047 Liu, C.-N., Lin, S.-F., Awasthi, A., Tsai, C.-J., Wu, Y.-C. and Chen, C.-F.: Sampling and  
 1048 conditioning artifacts of PM<sub>2.5</sub> in filter-based samplers, *Atmos. Environ.*, 85, 48–53, 2014.

1049 Liu, C.-N., Lin, S.-F., Tsai, C.-J., Wu, Y.-C. and Chen, C.-F.: Theoretical model for the  
 1050 evaporation loss of PM<sub>2.5</sub> during filter sampling, *Atmos. Environ.*, 109, 79–86, 2015.

1051 Liu, M., Huang, X., Song, Y., Tang, J., Cao, J., Zhang, X., Zhang, Q., Wang, S., Xu, T., Kang, L.,  
 1052 Cai, X., Zhang, H., Yang, F., Wang, H., Yu, J. Z., Lau, A. K. H., He, L., Huang, X., Duan, L.,  
 1053 Ding, A., Xue, L., Gao, J., Liu, B. and Zhu, T.: Ammonia emission control in China would  
 1054 mitigate haze pollution and nitrogen deposition, but worsen acid rain, *Proc. Natl. Acad. Sci. U.*  
 1055 *S. A.*, 116(16), 7760–7765, 2019.

1056 Liu, T., Clegg, S. L. and Abbatt, J. P. D.: Fast oxidation of sulfur dioxide by hydrogen peroxide  
 1057 in deliquesced aerosol particles, *Proc. Natl. Acad. Sci. U. S. A.*, 117(3), 1354–1359, 2020.

1058 Liu, X., Zhang, Y., Huey, L. G., Yokelson, R. J., Wang, Y., Jimenez, J. L., Campuzano-Jost, P.,  
 1059 Beyersdorf, A. J., Blake, D. R., Choi, Y., St. Clair, J. M., Crounse, J. D., Day, D. A., Diskin, G.  
 1060 S., Fried, A., Hall, S. R., Hanisco, T. F., King, L. E., Meinardi, S., Mikoviny, T., Palm, B. B.,  
 1061 Peischl, J., Perring, A. E., Pollack, I. B., Ryerson, T. B., Sachse, G., Schwarz, J. P., Simpson, I.  
 1062 J., Tanner, D. J., Thornhill, K. L., Ullmann, K., Weber, R. J., Wennberg, P. O., Wisthaler, A.,  
 1063 Wolfe, G. M. and Ziemba, L. D.: Agricultural fires in the southeastern U.S. during SEAC<sup>4</sup>RS:  
 1064 Emissions of trace gases and particles and evolution of ozone, reactive nitrogen, and organic  
 1065 aerosol, *J. Geophys. Res. D: Atmos.*, 121(12), 7383–7414, 2016.

1066 Liu, X., Huey, L. G., Yokelson, R. J., Selimovic, V., Simpson, I. J., Müller, M., Jimenez, J. L.,  
 1067 Campuzano-Jost, P., Beyersdorf, A. J., Blake, D. R., Butterfield, Z., Choi, Y., Crounse, J. D.,  
 1068 Day, D. A., Diskin, G. S., Dubey, M. K., Fortner, E., Hanisco, T. F., Hu, W., King, L. E.,  
 1069 Kleinman, L., Meinardi, S., Mikoviny, T., Onasch, T. B., Palm, B. B., Peischl, J., Pollack, I. B.,  
 1070 Ryerson, T. B., Sachse, G. W., Sedlacek, A. J., Shilling, J. E., Springston, S., St. Clair, J. M.,  
 1071 Tanner, D. J., Teng, A. P., Wennberg, P. O., Wisthaler, A. and Wolfe, G. M.: Airborne  
 1072 measurements of western U.S. wildfire emissions: Comparison with prescribed burning and air  
 1073 quality implications, *J. Geophys. Res. D: Atmos.*, 122(11), 6108–6129, 2017.

1074 Malm, W. C., Sisler, J. F., Huffman, D., Eldred, R. A. and Cahill, T. A.: Spatial and seasonal  
 1075 trends in particle concentration and optical extinction in the United States, *J. Geophys. Res.*,  
 1076 99(D1), 1347, 1994.

1077 Malm, W. C., Schichtel, B. A., Hand, J. L. and Collett, J. L., Jr.: Concurrent Temporal and  
 1078 Spatial Trends in Sulfate and Organic Mass Concentrations Measured in the IMPROVE  
 1079 Monitoring Program, *J. Geophys. Res. D: Atmos.*, 122(19), 10,462–10,476, 2017.

1080 Martin, N. A., Ferracci, V., Cassidy, N. and Hoffnagle, J. A.: The application of a cavity  
 1081 ring-down spectrometer to measurements of ambient ammonia using traceable primary standard  
 1082 gas mixtures, *Appl. Phys. B*, 122(8), 219, 2016.

1083 Ma, S.-S., Yang, W., Zheng, C.-M., Pang, S.-F. and Zhang, Y.-H.: Subsecond measurements on  
 1084 aerosols: From hygroscopic growth factors to efflorescence kinetics, *Atmos. Environ.*, 210,  
 1085 177–185, 2019.

1086 McNaughton, C. S., Clarke, A. D., Howell, S. G., Pinkerton, M., Anderson, B., Thornhill, L.,  
 1087 Hudgins, C., Winstead, E., Dibb, J. E., Scheuer, E. and Maring, H.: Results from the DC-8 Inlet  
 1088 Characterization Experiment (DICE): Airborne versus surface sampling of mineral dust and sea  
 1089 salt aerosols, *Aerosol Sci. Technol.*, 41(2), 136–159, 2007.

1090 Meskhidze, N., Chameides, W. L., Nenes, A. and Chen, G.: Iron mobilization in mineral dust:  
 1091 Can anthropogenic SO<sub>2</sub> emissions affect ocean productivity?, *Geophys. Res. Lett.*, 30(21), 2085,  
 1092 2003.

1093 Mezuman, K., Bauer, S. E. and Tsigaridis, K.: Evaluating secondary inorganic aerosols in three  
 1094 dimensions, *Atmos. Chem. Phys.*, 16(16), 10651–10669, 2016.

1095 Middlebrook, A. M., Bahreini, R., Jimenez, J. L. and Canagaratna, M. R.: Evaluation of  
 1096 Composition-Dependent Collection Efficiencies for the Aerodyne Aerosol Mass Spectrometer  
 1097 using Field Data, *Aerosol Sci. Technol.*, 46(3), 258–271, 2012.

1098 Müller, M., Mikoviny, T., Feil, S., Haidacher, S., Hanel, G., Hartungen, E., Jordan, A., Märk, L.,  
 1099 Mutschlechner, P., Schottkowsky, R., Sulzer, P., Crawford, J. H. and Wisthaler, A.: A compact  
 1100 PTR-ToF-MS instrument for airborne measurements of volatile organic compounds at high  
 1101 spatiotemporal resolution, , doi:10.5194/amt-7-3763-2014, 2014.

1102 Murphy, D. M. and Thomson, D. S.: Laser Ionization Mass Spectroscopy of Single Aerosol



- 1103 Particles, *Aerosol Sci. Technol.*, 22(3), 237–249, 1995.
- 1104 Murphy, D. M., Froyd, K. D., Schwarz, J. P. and Wilson, J. C.: Observations of the chemical  
1105 composition of stratospheric aerosol particles: The Composition of Stratospheric Particles, *Q.J.R.  
1106 Meteorol. Soc.*, 140(681), 1269–1278, 2014.
- 1107 Murray, B. J. and Bertram, A. K.: Inhibition of solute crystallisation in aqueous  
1108  $\text{H}^+ - \text{NH}_4^+ - \text{SO}_4^{2-} - \text{H}_2\text{O}$  droplets, *Phys. Chem. Chem. Phys.*, 10(22), 3287, 2008.
- 1109 Myhre, G., Shindell, D., Bréon, F.-M., Collins, W., Fuglestad, J., Huang, J., Koch, D.,  
1110 Lamarque, J.-F., Lee, D., Mendoza, B., Nakajima, T., Robock, A., Stephens, G., Takemura, T.  
1111 and Zhang, H.: Anthropogenic and Natural Radiative Forcing, in *Climate Change 2013: The  
1112 Physical Science Basis. Contribution of Working Group I to the Fifth Assessment Report of the  
1113 Intergovernmental Panel on Climate Change*, edited by T. F. Stocker, D. Qin, G.-K. Plattner, M.  
1114 Tignor, S. K. Allen, J. Boschung, A. Nauels, Y. Xia, V. Bex, and P. M. Midgley, p. 659,  
1115 Cambridge University Press, Cambridge, United Kingdom and New York, NY, USA., 2013.
- 1116 National Research Council: *The Airliner Cabin Environment and the Health of Passengers and  
1117 Crew*, The National Academies Press, Washington, DC., 2002.
- 1118 Nault, B. A., Campuzano-Jost, P., Day, D. A., Schroder, J. C., Anderson, B., Beyersdorf, A. J.,  
1119 Blake, D. R., Brune, W. H., Choi, Y., Corr, C. A., de Gouw, J. A., Dibb, J., DiGangi, J. P., Diskin,  
1120 G. S., Fried, A., Huey, L. G., Kim, M. J., Knute, C. J., Lamb, K. D., Lee, T., Park, T., Pusede, S.  
1121 E., Scheuer, E., Thornhill, K. L., Woo, J.-H. and Jimenez, J. L.: Secondary Organic Aerosol  
1122 Production from Local Emissions Dominates the Organic Aerosol Budget over Seoul, South  
1123 Korea, during KORUS-AQ, *Atmos. Chem. Phys.*, 18, 17769–17800, 2018.
- 1124 Nenes, A., Pandis, S. N., Kanakidou, M., Russell, A., Song, S., Vasilakos, P. and Weber, R. J.:  
1125 Aerosol acidity and liquid water content regulate the dry deposition of inorganic reactive  
1126 nitrogen, *Atmos. Phys. Chem. Discuss.*, doi:10.5194/acp-2020-266, 2020a.
- 1127 Nenes, A., Pandis, S. N., Weber, R. J. and Russell, A.: Aerosol pH and liquid water content  
1128 determine when particulate matter is sensitive to ammonia and nitrate availability, *Atmos. Chem.  
1129 Phys.*, 20(5), 3249–3258, 2020b.
- 1130 Nguyen, T. K. V., Zhang, Q., Jimenez, J. L., Pike, M. and Carlton, A. G.: Liquid water:  
1131 Ubiquitous contributor to aerosol mass, *Environ. Sci. Technol. Lett.*, 3, 257–263, 2016.
- 1132 Nie, W., Wang, T., Gao, X., Pathak, R. K., Wang, X., Gao, R., Zhang, Q., Yang, L. and Wang,  
1133 W.: Comparison among filter-based, impactor-based and continuous techniques for measuring  
1134 atmospheric fine sulfate and nitrate, *Atmos. Environ.*, 44(35), 4396–4403, 2010.
- 1135 Pagonis, D., Price, D. J., Algrim, L. B., Day, D. A., Handschy, A. V., Stark, H., Miller, S. L., de  
1136 Gouw, J., Jimenez, J. L. and Ziemann, P. J.: Time-Resolved Measurements of Indoor Chemical  
1137 Emissions, Deposition, and Reactions in a University Art Museum, *Environ. Sci. Technol.*,  
1138 53(9), 4794–4802, 2019.

1139 Paulot, F., Jacob, D. J., Johnson, M. T., Bell, T. G., Baker, A. R., Keene, W. C., Lima, I. D.,  
 1140 Doney, S. C. and Stock, C. A.: Global oceanic emission of ammonia: Constraints from seawater  
 1141 and atmospheric observations, *Global Biogeochem. Cycles*, 29(8), 1165–1178, 2015.

1142 Pratt, K. A. and Prather, K. A.: Aircraft measurements of vertical profiles of aerosol mixing  
 1143 states, *J. Geophys. Res.*, 115(D11), D11305, 2010.

1144 Price, H. C., Mattsson, J., Zhang, Y., Bertram, A. K., Davies, J. F., Grayson, J. W., Martin, S. T.,  
 1145 O’Sullivan, D., Reid, J. P., Rickards, A. M. J. and Murray, B. J.: Water diffusion in  
 1146 atmospherically relevant  $\alpha$ -pinene secondary organic material, *Chem. Sci.*, 6(8), 4876–4883,  
 1147 2015.

1148 Pye, H. O. T., Nenes, A., Alexander, B., Ault, A. P., Barth, M. C., Clegg, S. L., Collett, J. L., Jr.,  
 1149 Fahey, K. M., Hennigan, C. J., Herrmann, H., Kanakidou, M., Kelly, J. T., Ku, I.-T., McNeill, V.  
 1150 F., Riemer, N., Schaefer, T., Shi, G., Tilgner, A., Walker, J. T., Wang, T., Weber, R., Xing, J.,  
 1151 Zaveri, R. A. and Zuend, A.: The Acidity of Atmospheric Particles and Clouds, *Atmos. Chem.*  
 1152 *Phys.*, 20(8), 4809–4888, 2020.

1153 Robbins, R. C. and Cadle, R. D.: Kinetics of the Reaction between Gaseous Ammonia and  
 1154 Sulfuric Acid Droplets in an Aerosol, *J. Phys. Chem.*, 62(4), 469–471, 1958.

1155 Rumble, J. R., Ed.: *CRC Handbook of Chemistry and Physics*, 100th Edition, 2019 - 2020,  
 1156 Taylor & Francis Group., 2019.

1157 Schauer, C., Niessner, R. and Pöschl, U.: Polycyclic aromatic hydrocarbons in urban air  
 1158 particulate matter: decadal and seasonal trends, chemical degradation, and sampling artifacts,  
 1159 *Environ. Sci. Technol.*, 37(13), 2861–2868, 2003.

1160 Schroder, J. C., Campuzano-Jost, P., Day, D. A., Shah, V., Larson, K., Sommers, J. M., Sullivan,  
 1161 A. P., Campos, T., Reeves, J. M., Hills, A., Hornbrook, R. S., Blake, N. J., Scheuer, E., Guo, H.,  
 1162 Fibiger, D. L., McDuffie, E. E., Hayes, P. L., Weber, R. J., Dibb, J. E., Apel, E. C., Jaeglé, L.,  
 1163 Brown, S. S., Thornton, J. A. and Jimenez, J. L.: Sources and Secondary Production of Organic  
 1164 Aerosols in the Northeastern US during WINTER, *J. Geophys. Res. D: Atmos.*,  
 1165 doi:10.1029/2018JD028475, 2018.

1166 Seinfeld, J. H. and Pandis, S. N.: *Atmospheric Chemistry and Physics: From Air Pollution to*  
 1167 *Climate Change*, Second., John Wiley & Sons, Inc., Hoboken, NJ USA., 2006.

1168 Shingler, T., Crosbie, E., Ortega, A., Shiraiwa, M., Zuend, A., Beyersdorf, A., Ziemba, L.,  
 1169 Anderson, B., Thornhill, L., Perring, A. E., Schwarz, J. P., Campuzano-Jost, P., Day, D. A.,  
 1170 Jimenez, J. L., Hair, J. W., Mikoviny, T., Wisthaler, A. and Sorooshian, A.: Airborne  
 1171 characterization of subsaturated aerosol hygroscopicity and dry refractive index from the surface  
 1172 to 6.5 km during the SEAC<sup>4</sup> RS campaign, *J. Geophys. Res. D: Atmos.*, 121(8), 4188–4210,  
 1173 2016.

1174 Shiraiwa, M., Ammann, M., Koop, T. and Pöschl, U.: Gas uptake and chemical aging of

1175 semisolid organic aerosol particles, *Proc. Natl. Acad. Sci. U. S. A.*, 108(27), 11003–11008, 2011.

1176 Slade, J. H., Ault, A. P., Bui, A. T., Ditto, J. C., Lei, Z., Bondy, A. L., Olson, N. E., Cook, R. D.,  
 1177 Desrochers, S. J., Harvey, R. M., Erickson, M. H., Wallace, H. W., Alvarez, S. L., Flynn, J. H.,  
 1178 Boor, B. E., Petrucci, G. A., Gentner, D. R., Griffin, R. J. and Shepson, P. B.: Bouncier Particles  
 1179 at Night: Biogenic Secondary Organic Aerosol Chemistry and Sulfate Drive Diel Variations in  
 1180 the Aerosol Phase in a Mixed Forest, *Environ. Sci. Technol.*, 53(9), 4977–4987, 2019.

1181 Solomon, P. A., Mitchell, W., Tolocka, M., Norris, G., Gemmill, D., Wiener, R., Vanderpool, R.,  
 1182 Murdoch, R., Natarajan, S. and Hardison, E.: Evaluation of PM<sub>2.5</sub> Chemical Speciation  
 1183 Samplers for Use in the EPA National PM<sub>2.5</sub> Chemical Speciation Network, EPA., 2000.

1184 Solomon, P. A., Crumpler, D., Flanagan, J. B., Jayanty, R. K. M., Rickman, E. E. and McDade,  
 1185 C. E.: U.S. national PM<sub>2.5</sub> Chemical Speciation Monitoring Networks-CSN and IMPROVE:  
 1186 description of networks, *J. Air Waste Manag. Assoc.*, 64(12), 1410–1438, 2014.

1187 Song, S., Gao, M., Xu, W., Shao, J., Shi, G., Wang, S., Wang, Y., Sun, Y. and McElroy, M. B.:  
 1188 Fine-particle pH for Beijing winter haze as inferred from different thermodynamic equilibrium  
 1189 models, *Atmos. Chem. Phys.*, 18(10), 7423–7438, 2018.

1190 Spiller, L. L.: Determination of Ammonia/Air Diffusion Coefficient Using Nafion Lined Tube,  
 1191 *Anal. Lett.*, 22(11-12), 2561–2573, 1989.

1192 Stith, J. L., Ramanathan, V., Cooper, W. A., Roberts, G. C., DeMott, P. J., Carmichael, G., Hatch,  
 1193 C. D., Adhikary, B., Twohy, C. H., Rogers, D. C., Baumgardner, D., Prenni, A. J., Campos, T.,  
 1194 Gao, R., Anderson, J. and Feng, Y.: An overview of aircraft observations from the Pacific Dust  
 1195 Experiment campaign, *J. Geophys. Res.*, 114(D5), 833, 2009.

1196 Sueper, D.: ToF-AMS Data Analysis Software Webpage, [online] Available from:  
 1197 [http://cires1.colorado.edu/jimenez-group/wiki/index.php/ToF-AMS\\_Analysis\\_Software](http://cires1.colorado.edu/jimenez-group/wiki/index.php/ToF-AMS_Analysis_Software), 2018.

1198 Sun, K., Cady-Pereira, K., Miller, D. J., Tao, L., Zondlo, M. A., Nowak, J. B., Neuman, J. A.,  
 1199 Mikoviny, T., Müller, M., Wisthaler, A., Scarino, A. J. and Hostetler, C. A.: Validation of TES  
 1200 ammonia observations at the single pixel scale in the San Joaquin Valley during  
 1201 DISCOVER-AQ, *J. Geophys. Res. D: Atmos.*, 120(10), 5140–5154, 2015.

1202 Sun, Y., Zhang, Q., Macdonald, A. M., Hayden, K., Li, S. M., Liggio, J., Liu, P. S. K., Anlauf, K.  
 1203 G., Leaitch, W. R., Steffen, A., Cubison, M., Worsnop, D. R., van Donkelaar, A. and Martin, R.  
 1204 V.: Size-resolved aerosol chemistry on Whistler Mountain, Canada with a high-resolution aerosol  
 1205 mass spectrometer during INTEX-B, *Atmos. Chem. Phys.*, 9(9), 3095–3111, 2009.

1206 Sutton, M. A., Dragosits, U., Tang, Y. S. and Fowler, D.: Ammonia emissions from  
 1207 non-agricultural sources in the UK, *Atmos. Environ.*, 34(6), 855–869, 2000.

1208 Sutton, M. A., Reis, S., Riddick, S. N., Dragosits, U., Nemitz, E., Theobald, M. R., Tang, Y. S.,  
 1209 Braban, C. F., Viero, M., Dore, A. J., Mitchell, R. F., Wanless, S., Daunt, F., Fowler, D.,  
 1210 Blackall, T. D., Milford, C., Flechard, C. R., Loubet, B., Massad, R., Cellier, P., Personne, E.,

1211 Coheur, P. F., Clarisse, L., Van Damme, M., Ngadi, Y., Clerbaux, C., Skjøth, C. A., Geels, C.,  
 1212 Hertel, O., Wichink Kruit, R. J., Pinder, R. W., Bash, J. O., Walker, J. T., Simpson, D., Horváth,  
 1213 L., Misselbrook, T. H., Bleeker, A., Dentener, F. and de Vries, W.: Towards a climate-dependent  
 1214 paradigm of ammonia emission and deposition, *Philos. Trans. R. Soc. Lond. B Biol. Sci.*,  
 1215 368(1621), 20130166, 2013.

1216 Swartz, E., Shi, Q., Davidovits, P., Jayne, J. T., Worsnop, D. R. and Kolb, C. E.: Uptake of  
 1217 Gas-Phase Ammonia. 2. Uptake by Sulfuric Acid Surfaces, *J. Phys. Chem. A*, 103(44),  
 1218 8824–8833, 1999.

1219 Talbot, R. W., Dibb, J. E., Lefer, B. L., Scheuer, E. M., Bradshaw, J. D., Sandholm, S. T., Smyth,  
 1220 S., Blake, D. R., Blake, N. J., Sachse, G. W., Collins, J. E. and Gregory, G. L.: Large-scale  
 1221 distributions of tropospheric nitric, formic, and acetic acids over the western Pacific basin during  
 1222 wintertime, *J. Geophys. Res.: Atmos.*, 102(D23), 28303–28313, 1997.

1223 Tao, Y. and Murphy, J. G.: The sensitivity of PM<sub>2.5</sub> acidity to meteorological parameters and  
 1224 chemical composition changes: 10-year records from six Canadian monitoring sites, *Atmos.*  
 1225 *Chem. Phys.*, 19(14), 9309–9320, 2019.

1226 Thomson, D. S., Schein, M. E. and Murphy, D. M.: Particle Analysis by Laser Mass  
 1227 Spectrometry WB-57F Instrument Overview, *Aerosol Sci. Technol.*, 33(1-2), 153–169, 2000.

1228 Toon, O. B., Maring, H., Dibb, J., Ferrare, R., Jacob, D. J., Jensen, E. J., Luo, Z. J., Mace, G. G.,  
 1229 Pan, L. L., Pfister, L., Rosenlof, K. H., Redemann, J., Reid, J. S., Singh, H. B., Thompson, A.  
 1230 M., Yokelson, R., Minnis, P., Chen, G., Jucks, K. W. and Pszenny, A.: Planning, implementation,  
 1231 and scientific goals of the Studies of Emissions and Atmospheric Composition, Clouds and  
 1232 Climate Coupling by Regional Surveys (SEAC<sup>4</sup>RS) field mission, *J. Geophys. Res. D: Atmos.*,  
 1233 121(9), 4967–5009, 2016.

1234 Vay, S. A., Woo, J.-H., Anderson, B. E., Thornhill, K. L., Blake, D. R., Westberg, D. J., Kiley, C.  
 1235 M., Avery, M. A., Sachse, G. W., Streets, D. G., Tsutsumi, Y. and Nolf, S. R.: Influence of  
 1236 regional-scale anthropogenic emissions on CO<sub>2</sub> distributions over the western North Pacific, *J.*  
 1237 *Geophys. Res.*, 108(D20), 213, 2003.

1238 Vay, S. A., Choi, Y., Vadrevu, K. P., Blake, D. R., Tyler, S. C., Wisthaler, A., Hecobian, A.,  
 1239 Kondo, Y., Diskin, G. S., Sachse, G. W., Woo, J.-H., Weinheimer, A. J., Burkhardt, J. F., Stohl, A.  
 1240 and Wennberg, P. O.: Patterns of CO<sub>2</sub> and radiocarbon across high northern latitudes during  
 1241 International Polar Year 2008, *J. Geophys. Res.*, 116(D14), 4039, 2011.

1242 Walker, J. M., Philip, S., Martin, R. V. and Seinfeld, J. H.: Simulation of nitrate, sulfate, and  
 1243 ammonium aerosols over the United States, *Atmos. Chem. Phys.*, 12(22), 11213–11227, 2012.

1244 Wang, J., Hoffmann, A. A., Park, R. J., Jacob, D. J. and Martin, S. T.: Global distribution of solid  
 1245 and aqueous sulfate aerosols: Effect of the hysteresis of particle phase transitions, *J. Geophys.*  
 1246 *Res.*, 113(D11), 1770, 2008a.

1247 Wang, J., Jacob, D. J. and Martin, S. T.: Sensitivity of sulfate direct climate forcing to the

- 1248 hysteresis of particle phase transitions, *J. Geophys. Res.*, 113(D11), 13791, 2008b.
- 1249 Warneke, C., Schwarz, J. P., Ryerson, T., Crawford, J., Dibb, J., Lefer, B., Roberts, J., Trainer,  
1250 M., Murphy, D., Brown, S., Brewer, A., Gao, R.-S. and Fahey, D.: Fire Influence on Regional to  
1251 Global Environments and Air Quality (FIREX-AQ): A NOAA/NASA Interagency Intensive  
1252 Study of North American Fires, NOAA/NASA. [online] Available from:  
1253 <https://esrl.noaa.gov/csd/projects/firex-aq/whitepaper.pdf>, 2018.
- 1254 Warner, J. X., Wei, Z., Larrabee Strow, L., Dickerson, R. R. and Nowak, J. B.: The global  
1255 tropospheric ammonia distribution as seen in the 13-year AIRS measurement record, *Atmos.*  
1256 *Chem. Phys.*, 16(8), 5467–5479, 2016.
- 1257 Warner, J. X., Dickerson, R. R., Wei, Z., Strow, L. L., Wang, Y. and Liang, Q.: Increased  
1258 atmospheric ammonia over the world’s major agricultural areas detected from space, *Geophys.*  
1259 *Res. Lett.*, 44(6), 2875–2884, 2017.
- 1260 Watson, J. G., Chow, J. C., Chen, L. W. A. and Frank, N. H.: Methods to assess carbonaceous  
1261 aerosol sampling artifacts for IMPROVE and other long-term networks, *J. Air Waste Manag.*  
1262 *Assoc.*, 59(8), 898–911, 2009.
- 1263 Weber, R. J., Orsini, D., Daun, Y., Lee, Y.-N., Klotz, P. J. and Brechtel, F.: A Particle-into-Liquid  
1264 Collector for Rapid Measurement of Aerosol Bulk Chemical Composition, *Aerosol Sci.*  
1265 *Technol.*, 35(3), 718–727, 2001.
- 1266 Weber, R. J., Guo, H., Russell, A. G. and Nenes, A.: High aerosol acidity despite declining  
1267 atmospheric sulfate concentrations over the past 15 years, *Nat. Geosci.*, 9(4), 282–285, 2016.
- 1268 Williamson, C., Kupc, A., Wilson, J., Gesler, D. W., Reeves, J. M., Erdesz, F., McLaughlin, R.  
1269 and Brock, C. A.: Fast time response measurements of particle size distributions in the 3–60 nm  
1270 size range with the nucleation mode aerosol size spectrometer, *Atmos. Meas. Tech.*, 11(6),  
1271 3491–3509, 2018.
- 1272 Wilson, R. E.: Humidity Control by Means of Sulfuric Acid Solutions, with Critical Compilation  
1273 of Vapor Pressure Data, *J. Ind. Eng. Chem.*, 13(4), 326–331, 1921.
- 1274 Worsnop, D. R., Williams, L. R., Kolb, C. E., Mozurkewich, M., Gershenson, M. and  
1275 Davidovits, P.: Comment on “The NH<sub>3</sub> Mass Accommodation Coefficient for Uptake onto  
1276 Sulfuric Acid Solution,” *J. Phys. Chem. A*, 108(40), 8546–8548, 2004.
- 1277 Yao, X. H. and Zhang, L.: Supermicron modes of ammonium ions related to fog in rural  
1278 atmosphere, *Atmos. Chem. Phys.*, 12(22), 11165–11178, 2012.
- 1279 Zakoura, M., Kakavas, S., Nenes, A. and Pandis, S. N.: Size-resolved aerosol pH over Europe  
1280 during summer, *Atmos. Chem. Phys. Discuss.*, doi:10.5194/acp-2019-1146, 2020.
- 1281 Zhang, X., Smith, K. A., Worsnop, D. R., Jimenez, J., Jayne, J. T. and Kolb, C. E.: A Numerical  
1282 Characterization of Particle Beam Collimation by an Aerodynamic Lens-Nozzle System: Part I.

- 1283 An Individual Lens or Nozzle, *Aerosol Sci. Technol.*, 36(5), 617–631, 2002.
- 1284 Zhang, X., Smith, K. A., Worsnop, D. R., Jimenez, J. L., Jayne, J. T., Kolb, C. E., Morris, J. and  
1285 Davidovits, P.: Numerical Characterization of Particle Beam Collimation: Part II Integrated  
1286 Aerodynamic-Lens–Nozzle System, *Aerosol Sci. Technol.*, 38(6), 619–638, 2004.
- 1287 Zhou, S., Collier, S., Jaffe, D. A. and Zhang, Q.: Free tropospheric aerosols at the Mt. Bachelor  
1288 Observatory: more oxidized and higher sulfate content compared to boundary layer aerosols,  
1289 *Atmos. Chem. Phys.*, 19(3), 1571–1585, 2019.
- 1290